Hydrostratigraphic Mapping of the Surficial Aquifer System, Upper and Lower East Coast Planning Areas

Technical Publication WS-64

November 2024

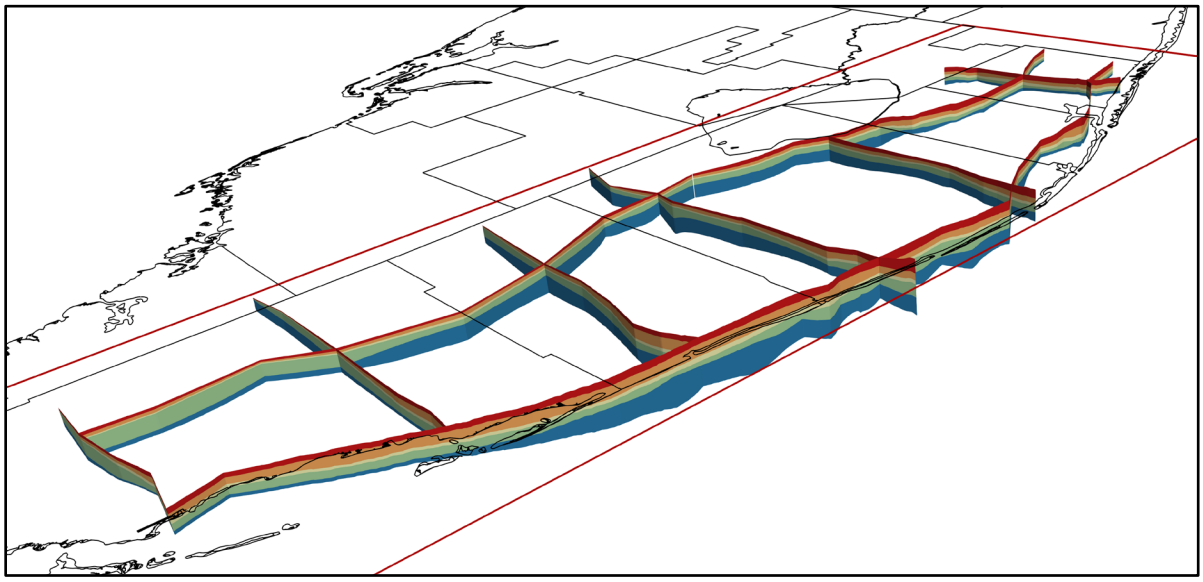

Stacey Coonts, P.G.
Water Supply Bureau, Water Resources Division

South Florida Water Management District | 3301 Gun Club Road | West Palm Beach, FL 33406

ACKLOWLEDGMENTS

The author would like to thank the Groundwater Modeling Unit of the South Florida Water Management District (SFWMD) Water Supply Bureau for sharing their expertise and support. In particular, the author wishes to express appreciation to Jefferson Giddings and David Butler for their contributions on compiling the data and Pete Kwiatkowski, P.G., Steve Krupa, P.G., and Justin Zumbro, P.G. for reviewing this report. The author also would like to thank Patricia Casey for providing technical editing of the final document.

EXECUTIVE SUMMARY

This document details the methods and results of mapping the hydrostratigraphy of the surficial aquifer system (SAS) in the South Florida Water Management District's (SFWMD or District) Upper East Coast (UEC) and Lower East Coast (LEC) planning areas. In addition to generally increasing the understanding of these aquifer systems, this study provides the basis for updating the model layers for the East Coast Surficial Model (ECSM), which is a density-dependent groundwater model. The study area corresponds with the ECSM model domain.

The objectives of this project were to create updated hydrostratigraphic surfaces for the SAS and to create hydrostratigraphic surface maps and isopach maps for each ECSM layer. The hydrostratigraphy was also rendered as a 3-dimensional (3-D) digital model and cross sections were made using this model. Hydrogeologic data sources used during this project include the SFWMD's corporate environmental database DBHYDRO and various Florida Geological Survey (FGS) and United States Geological Survey (USGS) publications.

Hydrostratigraphic layers correspond to the new ECSM layers. The ECSM layers are based on the Holocene sediments, the Quaternary (Q) units within the SAS, and the Pinecrest Sand Member and Ochopee Limestone Member of the Tamiami Formation. The data used to create these hydrostratigraphic layers, and the resulting surface and isopach rasters, have been archived in the SFWMD's Geographic Information System (GIS) files.

TABLE OF CONTENTS

1 Introduction 1

2 Geologic and Hydrogeologic Framework 3

2.1 Framework Background 3

2.2 Lithology and Stratigraphy 4

2.2.1 Holocene 4

2.2.2 Pleistocene 4

2.2.3 Pliocene 6

2.3 Hydrostratigraphy 6

2.3.1 Water Table Aquifer 6

2.3.2 Biscayne Aquifer 6

2.3.3 Semiconfining Unit 7

2.3.4 Turnpike Aquifer 7

2.3.5 Gray Limestone Aquifer 7

3 Data and Interpretation 7

4 Methods 8

4.1 Creation of Hydrostratigraphic Surfaces, a 3-D Hydrogeologic Model, and Hydrogeologic Cross Sections 8

5 Results 12

5.1 Isopach Maps and Hydrostratigraphic Surfaces 12

5.1.1 Layer 1 15

5.1.2 Layer 2 17

5.1.3 Layer 3 19

5.1.4 Layer 4 21

5.1.5 Layer 5 23

5.2 Hydrogeologic Cross Sections 26

6 Limitations and Recommendations 27

7 Literature Cited 28

Appendices 30

Appendix A: Data Used for Hydrostratigraphic Surface Creation A-1

Appendix B: Hydrogeologic Cross Sections B-1

LIST OF TABLES

Table 1. Summary of kriging methods and residuals for isopachs. 11
Table 2. Layer isopach map statistics. 13
Table 3. Layer hydrostratigraphic surface statistics. 13

LIST OF FIGURES

Figure 1. ECSM boundary and SFWMD planning regions and counties. 2
Figure 2. ECSM layers, Q units, stratigraphy, and hydrostratigraphy of the model area. 4
Figure 3. Example of a semivariogram plot 9
Figure 4. The different parts of a semivariogram plot. 9
Figure 5. Model fit lines in a semivariogram 10
Figure 6. Hydrostratigraphic layer fence diagrams produced using ParaView (100X vertical exaggeration). 12
Figure 7. Locations of lithological control used in this study. Linear feature in southern Miami-Dade County is the L-31N Cut-Off Wall investigation. 14
Figure 8. Layer 1 isopach map 15
Figure 9. Elevation of the top of Layer 1. 16
Figure 10. Layer 2 isopach map 17
Figure 11. Elevation of the top of Layer 2. 18
Figure 12. Layer 3 isopach map 19
Figure 13. Elevation of the top of Layer 3. 20
Figure 14. Layer 4 isopach map 21
Figure 15. Elevation of the top of Layer 4. 22
Figure 16. Layer 5 isopach map 23
Figure 17. Elevation of the top of Layer 5. 24
Figure 18. Elevation of the bottom of Layer 5 25
Figure 19. Hydrogeologic cross-sectional locations. 26
Figure 20. Cross section J-J'. 27

ACRONYMS AND ABBREVIATIONS

3-D	three dimensional
DBHYDRO	South Florida Water Management District's corporate environmental database for hydrologic, meteorologic, hydrogeologic, and water quality data
DEM	digital elevation model
District	South Florida Water Management District
ECSM	East Coast Surficial Model
FGS	Florida Geological Survey
ft	foot or feet
GIS	Geographic Information System
LEC	Lower East Coast
NAVD88	North American Vertical Datum of 1988
Q	Quaternary
SAS	surficial aquifer system
SFWMD	South Florida Water Management District
UEC	Upper East Coast
USGS	United States Geological Survey
WTA	Water Table aquifer

1 INTRODUCTION

The hydrostratigraphic mapping of the Upper East Coast (UEC) and Lower East Coast (LEC) planning areas was completed for the development of the East Coast Surficial Model (ECSM). **Figure 1** shows the boundary of the South Florida Water Management District (SFWMD or District) and its planning areas as well as the boundary of the ECSM. The study area corresponds with the ECSM extents. The purpose of this report is to share hydrostratigraphic surface and thickness (isopach) maps for the study area and cross sections of the regional hydrostratigraphy of the surficial aquifer system (SAS) based on these surfaces.

These hydrostratigraphic layers were determined using lithologic and geophysical data for 261 wells within the ECSM boundary. The resulting layer determinations in this report were utilized as the model layers for the ECSM. The ECSM is a density-dependent groundwater model and will evaluate the potential impacts of groundwater withdrawals in the SAS in the UEC and LEC for the next several decades. The population of these water supply planning areas is expected to increase, and new public supply projects will need to be developed. A comprehensive model that accurately reflects the regional hydrogeology is necessary for better planning to meet future water supply needs.

The hydrostratigraphy in this report and the new ECSM layers are based on the Quaternary (Q) units within the SAS. Q units are regional discontinuity surfaces that mark subaerial exposures during eustatic low sea level stands during the Pleistocene (Perkins 1977). The laminated crusts, organics, soils, and freshwater limestones that mark these low stands create thin layers of lower permeability that hydraulically separate the thicker and more permeable deposits that occur during marine high stands. Along with the Q units are the Holocene sediments and the Tamiami Formation. The Tamiami Formation is divided into the Pinecrest Sand Member and Ochopee Limestone Member.

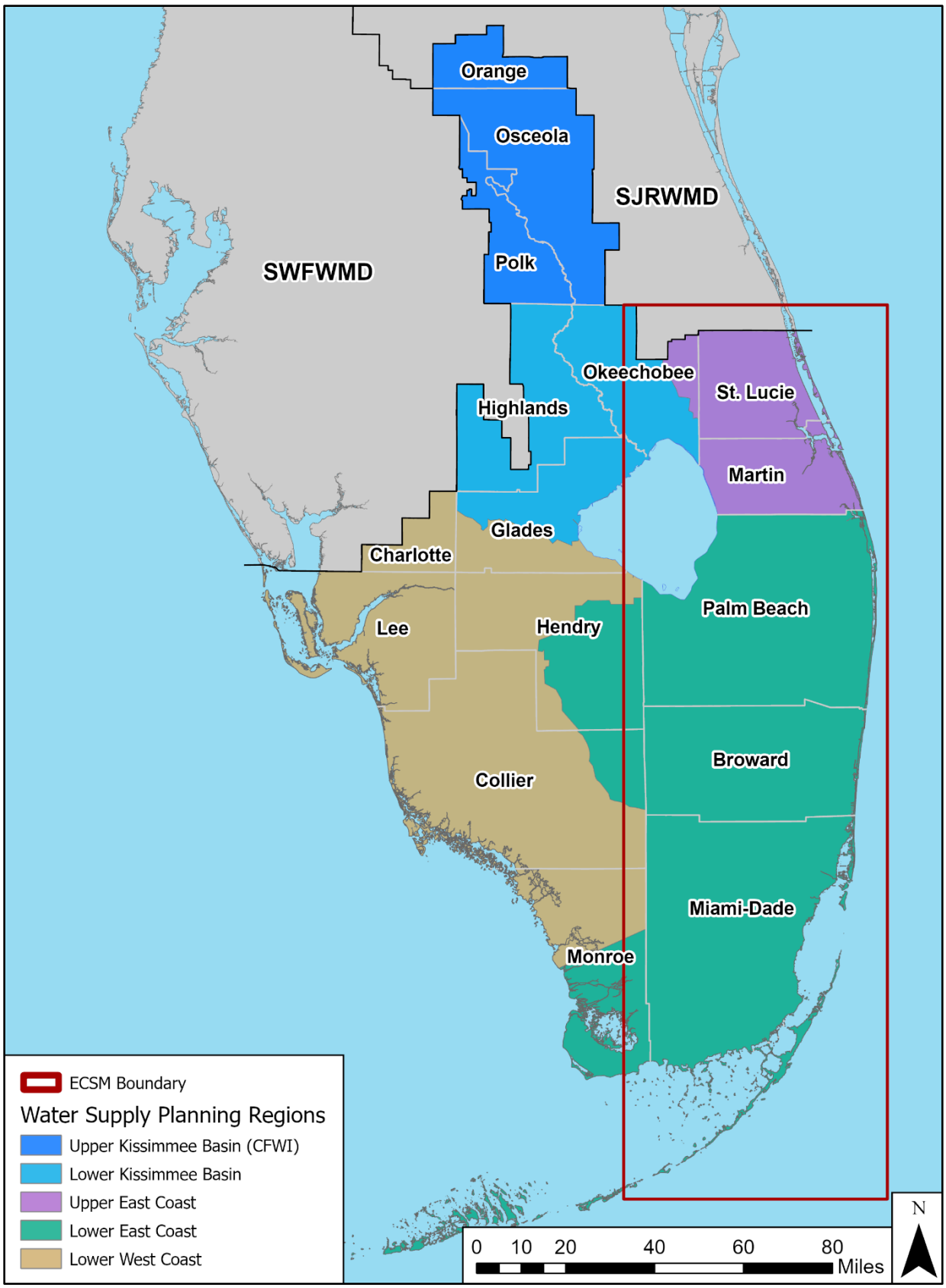

Figure 1. ECSM boundary and SFWMD planning regions and counties.

2 GEOLOGIC AND HYDROGEOLOGIC FRAMEWORK

2.1 Framework Background

The categorization of the sediments of the Pliocene and Pleistocene in Florida has long been discussed and debated. Due to the heterogenous lithology and frequent facies changes, classification of a specific formation can be difficult. The North America Stratigraphic Code requires that a geologic formation be defined "based on lithic characteristics and stratigraphic position." Consequently, a formation cannot be defined by the presence of specific shells or fossils. In the past, many of the Plio-Pleistocene formations of Florida were defined by the presence of specific fossils, thereby making these formations biostratigraphic formations. Currently, the Florida Geological Survey (FGS) uses the Shelly Sediments of Plio-Pleistocene Age as the lithostratigraphic unit name (Scott 2001) for nearly the entire SAS of South Florida. The stratigraphic units used in this report are the units used by the SFWMD and the United States Geological Survey (USGS).

The Holocene formations described in this report include undifferentiated soil and sand and the Lake Flirt Marl. The Pleistocene units include the Pamlico Sand, Miami Limestone, Fort Thompson Formation, Key Largo Limestone, Anastasia Formation, and Caloosahatchee Formation. The two members of the Tamiami Formation (the Pinecrest Sand Member and Ochopee Limestone Member) comprise the Pliocene units of South Florida. These sediments and rocks make up the SAS, which can be further subdivided into the Water Table aquifer (WTA), Biscayne aquifer, semiconfining unit, Turnpike aquifer, and Gray Limestone aquifer, depending on location. The SAS is underlain by the intermediate aquifer system, which was not mapped as part of this report.

The deposition of the clastic and carbonate sediments that form the SAS was driven by the eustatic sea level changes that occurred during the numerous glacial and interglacial stages of the Pleistocene. These sea level changes resulted in regressive and transgressive sediment depositional cycles that can be identified throughout the SAS using sequence stratigraphic methods. Within Pleistocene formations, deposition primarily occurred during high sea level stands that submerged the carbonate platform. These marine deposits include coral reefs, marine invertebrates, saltwater limestone, and oolites. Erosion of these deposits occurred during subaerial exposures during periods of lower sea levels. The subaerial erosional surfaces can be identified based on the presence of paleosols, soil breccias, root structures, laminated crusts, solution surfaces, and freshwater limestones (Perkins 1977). Perkins (1977) used these marine deposits and erosional surfaces to separate the Pleistocene sediments of South Florida into five geologic units named Q1, Q2, Q3, Q4, and Q5, with Q1 being the oldest and Q5 being the youngest.

Multiple subaerial exposure surfaces have been identified in the Miami Limestone, Fort Thompson Formation, Key Largo Limestone, Anastasia Formation, and Caloosahatchee Formation. The erosional surfaces that bound each of the Q units are important features of the geologic model because the soil and laminated crusts that compose the subaerial exposure surfaces identified between each of the Q units generally are composed of fine-grained sediments that have lower permeability than the underlying lithologic formation. Although thin, these low-permeability exposure surfaces affect horizontal and vertical groundwater flow and divide formations into multiple flow zones (Wacker et al. 2014). The model layers should show these multiple flow zones and include the effects they have on horizontal and vertical groundwater flow. Laminated crusts or caliche that were deposited during subaerial exposure or at the top of paleo groundwater interfaces often contain elevated concentrations of precipitated radioactive minerals or elements that are incorporated into the fine-grained sediments deposited during exposure. These radioactive materials cause distinct increases in gamma-ray geophysical log responses that can be combined with lithologic observations to determine the elevation of individual Q surfaces (Reese and Wacker 2007).

2.2 Lithology and Stratigraphy

The lithology and stratigraphy of the east coast of South Florida is outlined in this section. **Figure 2** provides a summary of the stratigraphy and its relation to geologic age, model layers, Q units, and hydrostratigraphy.

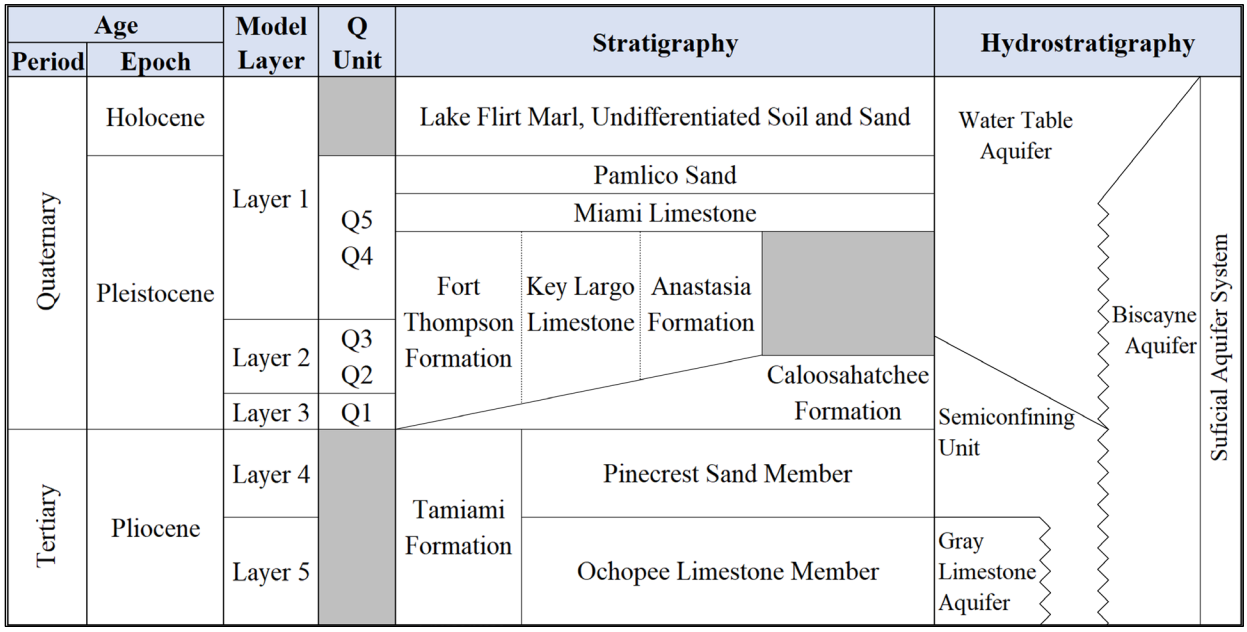

Figure 2. ECSM layers, Q units, stratigraphy, and hydrostratigraphy of the model area.

2.2.1 Holocene

Holocene sediments are the youngest sediments included in this study and are composed of undifferentiated sand, organic soil, and peat that were deposited in beach, dune, marsh, and lagoon environments during the most recent sea level high stand. Underlying these undifferentiated sediments is the Lake Flirt Marl, which consists of shelly marl and organic-rich sands. Freshwater gastropods, such as *Planorbella,* are abundant (DuBar 1962). Where present, the Holocene sediments overlie the Pamlico Sand and other Pleistocene deposits (Cooke 1945).

2.2.2 Pleistocene

The Pleistocene deposits of South Florida include the Pamlico Sand, Miami Limestone, Fort Thompson Formation, Key Largo Limestone, Anastasia Formation, and Caloosahatchee Formation. These Pleistocene deposits are primarily composed of shallow-water marine carbonates and clastics that have undergone several cycles of subaerial exposures during multiple sea level changes. Lithologic evidence of these subaerial exposures includes laminated crusts, root casts, and freshwater limestones (Perkins 1977). The Fort Thompson Formation, Key Largo Limestone, and Anastasia Formation were formed contemporaneously and are essentially different facies that were deposited across a laterally extensive area.

2.2.2.1 Pamlico Sand

During the late Pleistocene, quartz sand was deposited as beach sand in South Florida through longshore transport. The Pamlico Sand was deposited in most of the region south of Lake Okeechobee. It is composed mostly of sand with some clay but includes all the marine Pleistocene deposits younger than the Anastasia Formation. The top of the Pamlico Sand rarely extends above 25 feet above sea level, which was the

approximate elevation of the shoreline during the third interglacial stage (Parker and Cooke 1944). The Pamlico Sand is characterized by a paucity of fossils, particularly mollusks. The Pamlico Sand is part of the Q5 unit and overlies the Miami Limestone, Fort Thompson Formation, and Anastasia Formation. It is overlain by the Lake Flirt Marl and Holocene sediments.

2.2.2.2 Miami Limestone

The Miami Limestone forms the southern end of the Atlantic Coastal Ridge and underlies the southern portion of the Everglades. It is composed of two facies, an upper oolitic facies and a lower *Schizolle floridana* bryozoan facies (Hoffmeister et al. 1967). The Miami Limestone was deposited during Q4 and Q5 and transitions into the upper sections of the Fort Thompson Formation and Anastasia Formation to the north and into the upper sections of the Key Largo Limestone to the south.

2.2.2.3 Fort Thompson Formation

The Fort Thompson Formation is a lithologically variable formation that was deposited concurrently with the Anastasia Formation and the Key Largo Limestone. It interfingers with these two formations to the east and south, respectively. The Fort Thompson Formation is composed of marine limestone, freshwater limestone, quartz sandstone, and sandy limestone. It is highly fossiliferous, with extensive shell debris composed primarily of mollusks, including *Chione cancellata* (Petuch and Roberts 2007). The Fort Thompson Formation contains all of the Q units.

2.2.2.4 Key Largo Limestone

The Key Largo Limestone is a coralline limestone with minor amounts of sandy limestone that is exposed on Key Largo, Florida. The upper section of this stratigraphic unit transitions into the Miami Limestone along the western edge of Biscayne Bay. The most prevalent corals are *Porites, Diplora,* and *Monastrea,* which indicate an inner reef depositional environment (Hoffmeister 1974). The Key Largo Limestone contains all of the Q units.

2.2.2.5 Anastasia Formation

The Anastasia Formation was deposited in a high energy beach/barrier island environment restricted to the east coast of Florida. The Anastasia Formation forms the majority of the Atlantic Coastal Ridge and is exposed at the surface in several areas. This marine deposit is composed of interbedded, sandy molluscan coquina and shelly quartz sand beds. The mollusk shells are fragmented and abraded. Barnacles are common (Petuch and Roberts 2007). The Anastasia Formation interfingers with the Fort Thompson Formation to the west. The Anastasia Formation has two subaerial surfaces and contains all of the Q units.

2.2.2.6 Caloosahatchee Formation

The Caloosahatchee Formation consists of thin sequences of interbedded clay, marl, silt, and sand containing locally abundant shells and shell fragments (Miller 1986). The formation extends from the west coast of Florida to about the western half of the study area. Where present, the Caloosahatchee Formation unconformably overlies the Tamiami Formation and underlies the Fort Thompson Formation. The Caloosahatchee Formation was deposited during Q1 and Q2.

2.2.3 Pliocene

2.2.3.1 Tamiami Formation

The Tamiami Formation is a lithologically diverse formation that has undergone several changes to its definition and age since its initial naming by Mansfield (1939). Hunter and Wise (1980) proposed that the Tamiami Formation was composed of the Ochopee Limestone, the Buckingham Limestone, and the Pinecrest Sand, with the previously defined members of the lower Tamiami Formation being reassigned to the underlying Peace River Formation. This study follows their definition, though only the Pinecrest Sand Member and the Ochopee Limestone Member were identified in the wells used in this report.

2.2.3.1.1 Pinecrest Sand Member

The Pinecrest Sand Member is predominantly a light gray to olive gray well-sorted quartz sand with abundant well-preserved shell fossils (Reese and Cunningham 2000). Minor amounts of phosphate grains and heavy minerals found in the Pinecrest Sand are the result of reworking of Hawthorn Group sediments (Scott 1988). Rudstone, floatstone, and mudstone are rare, but found as thin beds within the Pinecrest Sand.

2.2.3.1.2 Ochopee Limestone Member

The Ochopee Limestone Member is a gray to dark gray, moldic, well-indurated, bivalve-rich rudstone and floatstone (Reese and Cunningham 2000). It also commonly contains abundant fine quartz sand layers, with the stratigraphic unit's sand content increasing with depth. The Ochopee Limestone Member also contains thin beds of bivalve-rich quartz sand or sandstone. The bivalves commonly found are oysters, *Pecten, Chione,* and *Ostrea*. Phosphate can be present in minor amounts but at lower concentrations than the Pinecrest Sand. The base of the Ochopee Limestone Member is the base of the SAS within this study area.

2.3 Hydrostratigraphy

The hydrogeology of South Florida is also complex. Due to the horizontally and vertically heterogenous nature of the lithologies that compose the regional hydrostratigraphy, contemporaneous lithostratigraphic units can be confining in one area and a productive aquifer in others. Within the SAS in the study area, three aquifers are defined. These are the WTA, Biscayne aquifer, and Gray Limestone aquifer. These aquifers locally grade into one another and can be hydraulically connected with each other.

2.3.1 Water Table Aquifer

The WTA is composed of sand, limestone, sandstone, and coquina. It is sometimes underlain by a confining unit but can also be hydraulically connected to the underlying Gray Limestone aquifer. It is predominantly composed of Holocene sediments and Q1 through Q5 units. The WTA comprises ECSM Layer 1, Layer 2, and sometimes Layer 3. In model Layer 3 (also Q1), this unit can be semiconfining in areas where the clayey and marly Caloosahatchee Formation or lower portion of the Fort Thompson Formation are present. Along the coast where coquina of the Anastasia Formation is present and hydraulic conductivity is higher, model Layer 3 is part of the WTA.

2.3.2 Biscayne Aquifer

The Biscayne aquifer covers the southeast portion of the study area, including southeastern Monroe County and Palm Beach County, and nearly all of Miami-Dade and Broward counties. It is predominantly composed of the Miami Limestone and Fort Thompson Formation (Wacker et al. 2014). The Biscayne aquifer includes all five Q units, and ECSM Layers 1, 2, and 3. Along the east coast of Broward and

Miami-Dade counties and the southeast corner of Palm Beach County, ECSM Layers 4 and 5 are more permeable than to the east and are included in the Biscayne aquifer.

2.3.3 Semiconfining Unit

Confinement between the Gray Limestone aquifer and the Biscayne aquifer or WTA comes from the semiconfining unit. The semiconfining unit includes portion of ECSM Layers 3 and 4. Layer 3 in western Palm Beach, Martin, and St. Lucie counties as well as Okeechobee County is composed of the clayey and marly Caloosahatchee Formation or lower portion of the Fort Thompson Formation. ECSM Layer 4 is the Pinecrest Sand Member of the Tamiami Formation, which is semiconfining except along the coastline of Palm Beach County, Broward County, and the northeast portion of Miami-Dade County.

2.3.4 Turnpike Aquifer

In Reese and Wacker (2009), the term "Turnpike aquifer" was proposed for this zone because it was identified near the Florida Turnpike. As discussed in Section 2.3.3, ECSM Layer 4 is the Pinecrest Sand Member of the Tamiami Formation and is primarily a semiconfining unit above the Gray Limestone aquifer across the study area. Along the coastline of Palm Beach County, Broward County, and the northeast portion of Miami-Dade County, this layer is permeable. The increased permeability comes from interconnected vugs and molds.

2.3.5 Gray Limestone Aquifer

The Gray Limestone aquifer is composed of the sandy, bivalve-rich, gray rudstone and floatstone of the Ochopee Limestone Member of the Tamiami Formation (Reese and Cunningham 2000). The Gray Limestone aquifer is present beneath eastern and central Collier County, southern Hendry County, and western Palm Beach, Broward, and Miami-Dade counties. It is equivalent to the Lower Tamiami aquifer to the north and west (Reese and Cunningham 2000). In areas where it is not semiconfined or confined, it is hydraulically connected to the WTA and/or Biscayne aquifer. The Gray Limestone aquifer is equivalent to ECSM Layer 5.

3 DATA AND INTERPRETATION

Multiple sources of data were reviewed prior to being included in this study and the ECSM. The District's corporate environmental database, DBHYDRO, was used to obtain information about well locations, lithology, aquifer performance tests, and geophysical logs. In addition, the FGS lithology database GEODES was used to obtain some of the lithologic logs. Publications from the SFWMD, FGS, and USGS as well as consultant reports were also reviewed.

High-quality geologic and hydrogeologic data were included in the ECSM only if the Q units and the members of the Tamiami Formation could be determined. Lithologic logs that described features indicative of low sea stands, identified diagnostic fossils, and described lithology in intervals of 10 feet or less were preferred. The resulting data set used to develop the hydrostratigraphic layers was composed of 263 points. Of these, 261 points were wells, and 2 were "ghost points." A method called kriging, explained further in Section 4.1, was used to mathematically estimate continuous datasets through the study area using the well data points. The ghost points were necessary to constrain the kriging program to the ECSM model extent, (one in the farthest northwestern extent and one in the farthest southeastern extent) and are not real wells.

When evaluating lithology, evidence of high and low sea level stands was utilized to determine the Q units. Following guidance from Perkins (1977), the geologic features indicative of low sea level stands are organics, root structures, laminated crusts, paleosols, solution surfaces, and freshwater limestones. The

discontinuity surfaces commonly have red iron staining or brown and black coloration due to the presence of organic matter. Fossils of terrestrial gastropods, such as *Helisoma,* can be found within the freshwater limestones.

High sea level stands are marked by periods of high rates of deposition and the presence of marine fossils, including bryozoans, corals (e.g., *Montastra*, *Diploria*, and *Porites*) and mollusks, such as *Chione* and *Rangia*, oysters, and scallops. When available, optical borehole imaging and geophysical logs were used in conjunction with lithologic information to identify the discontinuity surfaces.

4 METHODS

4.1 Creation of Hydrostratigraphic Surfaces, a 3-D Hydrogeologic Model, and Hydrogeologic Cross Sections

Numerous software was utilized for the creation of hydrostratigraphic surfaces, a 3-D hydrogeologic model, and cross sections. These include Surfer version 25.1.229 (Golden Software 2023), Python, ParaView version 5.11.2 (Kitware 2023), and ArcMap version 10.8.1 (ESRI 2020), including ArcGIS 3-D Analyst extension and ArcScene. Surfer was used for kriging the isopach rasters using the raw data. A Python script was created to automate the creation process of the elevation rasters, contours, and other Geographic Information System (GIS) data within ArcMap. The raster grids contain 313 columns and 1,060 rows. Each raster cell is 1,000 feet by 1,000 feet with an origin at the lower left corner of the groundwater model domain in State Planar Coordinates (NAD 1983 HARN Florida East FIPS_0901, feet) of 671,436.8, 142,755.9 (82°32'38.59" W, 24°30'36.76" N).

Kriging has been used by the District in the past for mapping hydrostratigraphic surfaces (Geddes et al. 2015, Zumbro et al. 2023) and was used again for this study. Some interpolation methods, such as the inverse distance weighted method, weights each data point based only on the distance from the point being estimated. Kriging, however, considers a more complex relationship of how weights change with distance. Kriging also accounts for directionality and compensates for effects such as data clustering. This makes kriging particularly useful when interpolating geologic surfaces because geologic units are commonly affected by directionality. Specifically, the geologic units are affected by and often deposited based upon the effects of wind and water and resultant sorting of sediments. Kriging can also handle the clustering effect of having more wells constructed in higher population areas than in rural areas. The mathematical relationship of how weights change with distance is determined through creating a semivariogram. A semivariogram is created by pairing every point in a data set with every other point of that same data set. Each data point pair is then graphed using the distance between the points and semivariance. An example of a semivariogram plot is shown in **Figure 3** and discussed further below. Semivariance is the squared difference of the values of the point pairs as shown in **Equation 1**:

$$\gamma = \frac{1}{2}(v_i - v_j)^2 \qquad \text{Equation 1}$$

where:

γ = semivariance

v_i = value of the first point in a point pair

v_j = value of the second point in a point pair

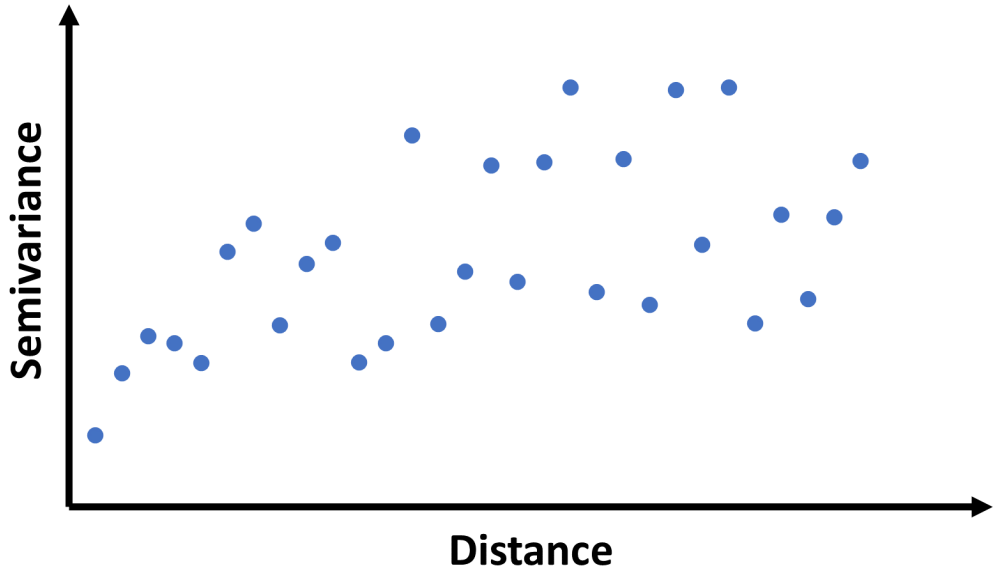

Figure 3. Example of a semivariogram plot.

The semivariogram works on the principle that data points located close to one another are more related and have a smaller semivariance than points located farther away from one another. Point pairs separated by a short distance are expected to have low semivariance, while point pairs that are far apart are expected to have a higher semivariance. At a certain distance, the semivariance levels off. The distance where this occurs is called the range. The value of the leveled off semivariance is called the sill. The y-intercept of the semivariogram is known as the nugget, and it accounts for errors and uncertainty in the data. It shows the level of semivariance possible for a point pair at the same location or in the same model cell (Kitanidis 1997). The different parts of a semivariogram plot are depicted below in **Figure 4**.

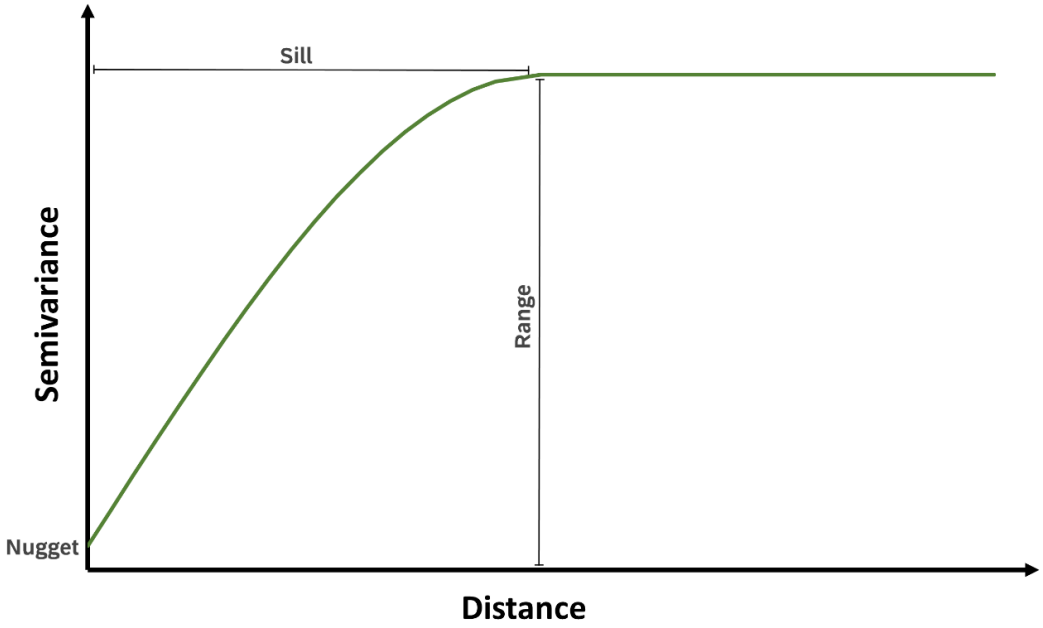

Figure 4. The different parts of a semivariogram plot.

Using the semivariogram plot, a best-fit model (e.g., spherical, exponential, linear) can then be fit to the semivariogram data points. **Figure 5** is an example of the shape of the best-fit lines for different model types. Once a best-fit model is selected, it is used during the kriging process to calculate values in cells with unknown values.

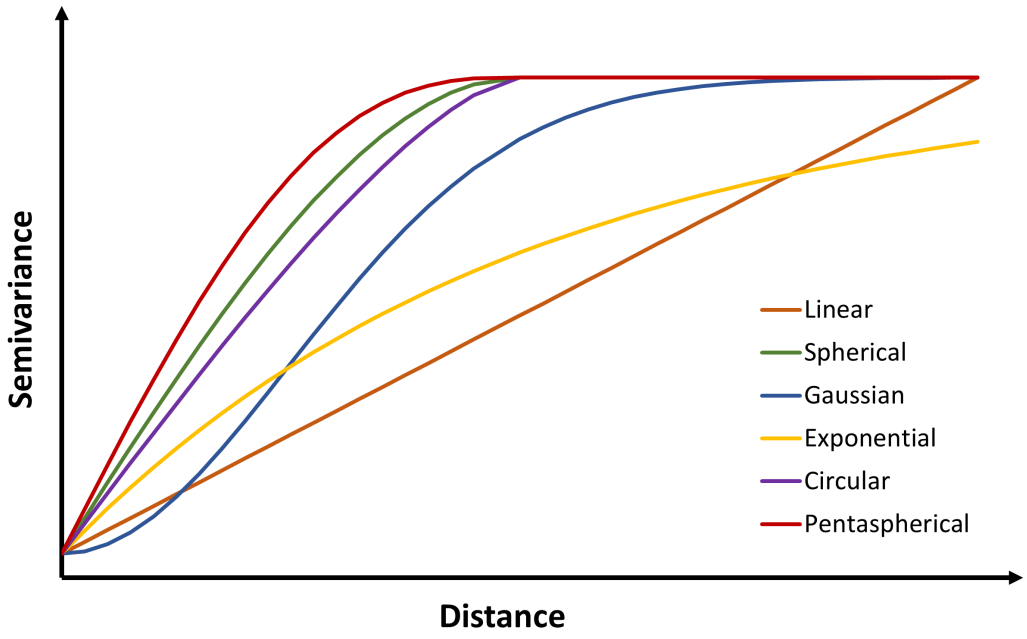

Figure 5. Model fit lines in a semivariogram.

The search neighborhood settings used during the kriging process determine which data points will be used when calculating the value for a point without a known value. This can be a minimum number of nearby points or all points within a certain search radius. The search neighborhood allows for calculations to be made using local values rather than using all point pairs in a data set to calculate one cell value. Using local values increases the speed of kriging by only calculating weights for the nearest points. The weighted values of points far away have negligible influence on the estimation and do not need to be calculated.

Cross-validation is important for evaluation of a kriged raster. Cross-validation removes one input data point at a time from the data set and predicts the output values for those locations using the rest of the data set. The predicted and omitted actual values are then compared, and the error is calculated. Cross-validation that shows a small error between the input and predicted values means that the model was well fit to the data (GISGeography 2022).

Surfer was chosen as the kriging software because it allows for adjustments to the semivariogram, adjustments to the search neighborhoods, and cross-validation. Surfer could not be automated with Python but allowed the user to set limits for maximum and minimum values of the output isopach maps. These limits prevented the kriging process from overestimating or underestimating a value that went beyond the input data set's range. For example, a minimum input thickness of 1-foot resulted in isopachs that were not thinner than 1 foot.

ECSM layer thicknesses were kriged first. Next, the elevations of the tops of each model layer and the bottom of the deepest model layer were calculated. This order was chosen so that there would not be any negative thicknesses that would cause layers to intersect each other. Once the thicknesses were interpolated for each model layer, the elevations of each layer were calculated by subtracting the thickness of each layer from the ground surface elevation.

Residuals were then calculated to evaluate the quality of the rasters created. Residuals are calculated by calculating the difference between the observed input values and model prediction values at those same locations. If the residuals are normally distributed, have a small standard deviation, and have a mean of zero, then the model has done a good job of matching the observed values. The initial rasters drawn using Surfer with a nugget of zero had nearly zero residuals for all ECSM layers but had a "spikey" appearance when viewed in 3-D using ESRI's ArcScene. Cross sections and fence diagrams of the Surfer surfaces showed a bowing effect in areas between wells, which is not consistent with natural sedimentary depositional processes.

Adjusting the nugget was found to be the solution to Surfer's unrealistic, spikey surface output. The nugget is the y-intercept of a model fit line in a semivariogram. The nugget comes from the error and uncertainty in the data. In hydrogeologic data, these errors can come from well location, data quality (e.g., cuttings interval, level of detail in lithologic logs), and uncertainties in the hydrostratigraphic/aquifer selections (e.g., gradational contacts, differences in professional interpretation). The final rasters were created in Surfer using a larger nugget value of 15. The kriging methods and summary of residuals for each of the model layers are provided in **Table 1**.

Table 1. Summary of kriging methods and residuals for isopachs.

Model Layer	Kriging Method	Mean Residual	Standard Deviation Residual
Layer 1	Exponential	1.32	8.83
Layer 2	Exponential	0.29	9.00
Layer 3	Spherical	0.81	4.97
Layer 4	Exponential	0.68	9.87
Layer 5	Spherical	0.44	13.28

The isopach maps and elevation rasters were converted to triangular irregular network files and reviewed in 3-D using ArcScene. Viewing the data in 3-D allowed the hydrostratigraphic surfaces and isopachs to be further refined and checked in greater detail than the 2-D images allowed. The hydrogeologic cross sections and fence diagrams were created using the PyVista library of Python. PyVista converted the 2-D rasters into 3-D blocks and sliced them along the cross-sectional lines. The resulting slices were prepared for publishing using ParaView. The fence diagrams are shown below in **Figure 6**.

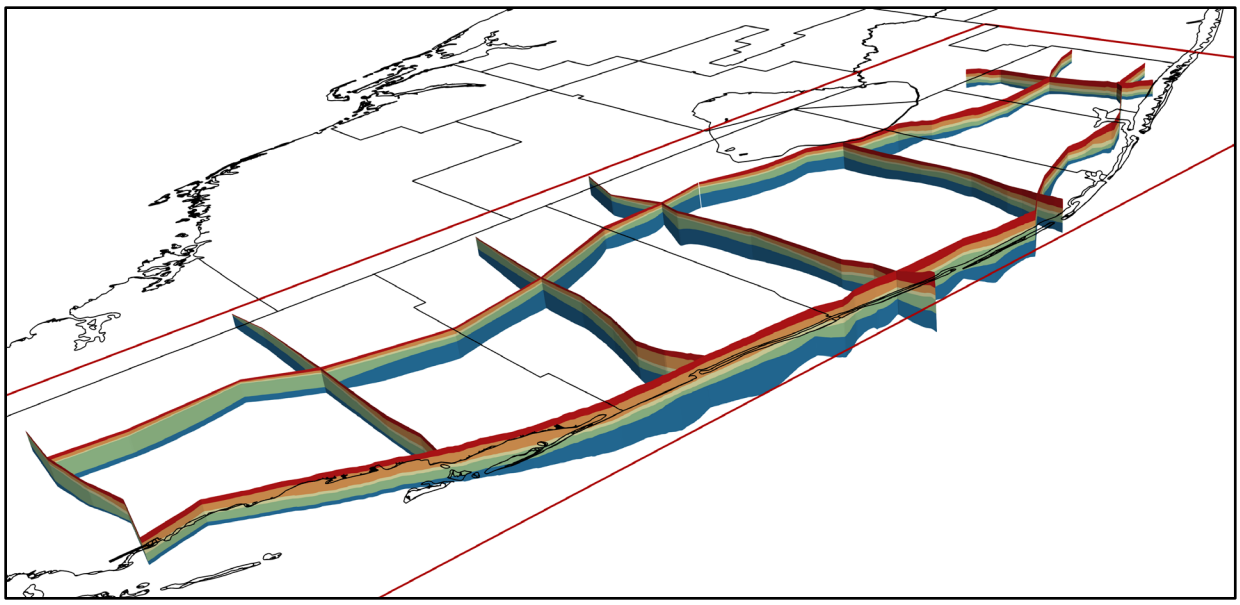

Figure 6. Hydrostratigraphic layer fence diagrams produced using ParaView (100X vertical exaggeration).

5 RESULTS

The following sections present the results of the creation of isopach maps and hydrostratigraphic surfaces as well as hydrogeologic cross sections.

5.1 Isopach Maps and Hydrostratigraphic Surfaces

Isopach maps were generated for each ECSM layer. Hydrostratigraphic surfaces for the tops of each layer and the bottom of Layer 5 (except for the top of Layer 1 where the top was assumed to be land surface) were created by subtracting those layer thicknesses from land surface. A raster of land surface in feet North American Vertical Datum of 1988 (NAVD88) was created using ArcMap by resampling a 1-foot digital elevation model (DEM) of the best available data within the study area. The original DEM (SFWMD Districtwide Digital Elevation Model, obtained from SFWMD Geospatial Services) was composited in 2020 from multiple sources. The 5-foot by 5-foot cell size of the DEM was resampled to a grid size of 1,000 feet by 1,000 feet corresponding to the model grid. Landfills were filtered out of the topography because they result in large, artificial elevation highs that do not correspond with the natural top of the topography. For example, the Monarch Hill Renewable Energy Park located in northeastern Broward County, is 225 feet tall at its highest point. This landfill covers 15 model cells. Calculating the top of the subsequent layers with an artificial elevation nearly 200 feet higher than the elevation in nearby cells results in incorrect elevations for other layers that put the tops of those layers within the landfill's mound. Flattening these tall landfills in the topography layer prevents these errors. Statistical summaries of the isopach maps and hydrostratigraphic surfaces are provided in **Tables 2** and **3**, respectively.

Table 2. Layer isopach map statistics.

Model Layer	Number of Data Points	Minimum Thickness, feet	Maximum Thickness, feet	Mean Thickness, feet	Standard Deviation
1	263	3	118	25.8	13.6
2	263	2	110	26.2	16.4
3	263	1	49	13.8	7.9
4	263	1	120	43.2	20.4
5	263	1	208	59.6	33.9

Table 3. Layer hydrostratigraphic surface statistics.

Model Layer	Surface	Min Elevation, feet NAVD88	Max Elevation, feet NAVD88	Mean Elevation, feet NAVD88	Standard Deviation
1	Top	-1.6	73.8	12.8	12.2
2	Top	-86.8	34.9	-13.0	13.0
3	Top	-134.8	8.0	-39.6	24.5
4	Top	-158.8	6.1	-53.4	29.2
5	Top	-240.7	-1.7	-97.7	32.1
5	Bottom	-379.5	-67.7	-157.3	46.1

NAVD88 = North American Vertical Datum of 1988.

Figure 7 is a map depicting the locations of the wells and ghost points. Each well had data for all 5 layers. Generally, there are more points in areas of higher population and near the coastline. The points in the farthest northwestern and southeastern extents are ghost points added for the purpose of constraining the kriging program Surfer to the desired extent. The well names, state plane coordinates, land surface elevation, and the thicknesses of model layers at each well are provided in **Appendix A**. In southern Miami-Dade County, the line of densely spaced wells is the series of wireline core borings drilled as part of the L-31N Cut-Off Wall investigation. These borings run along the L-31N Levee.

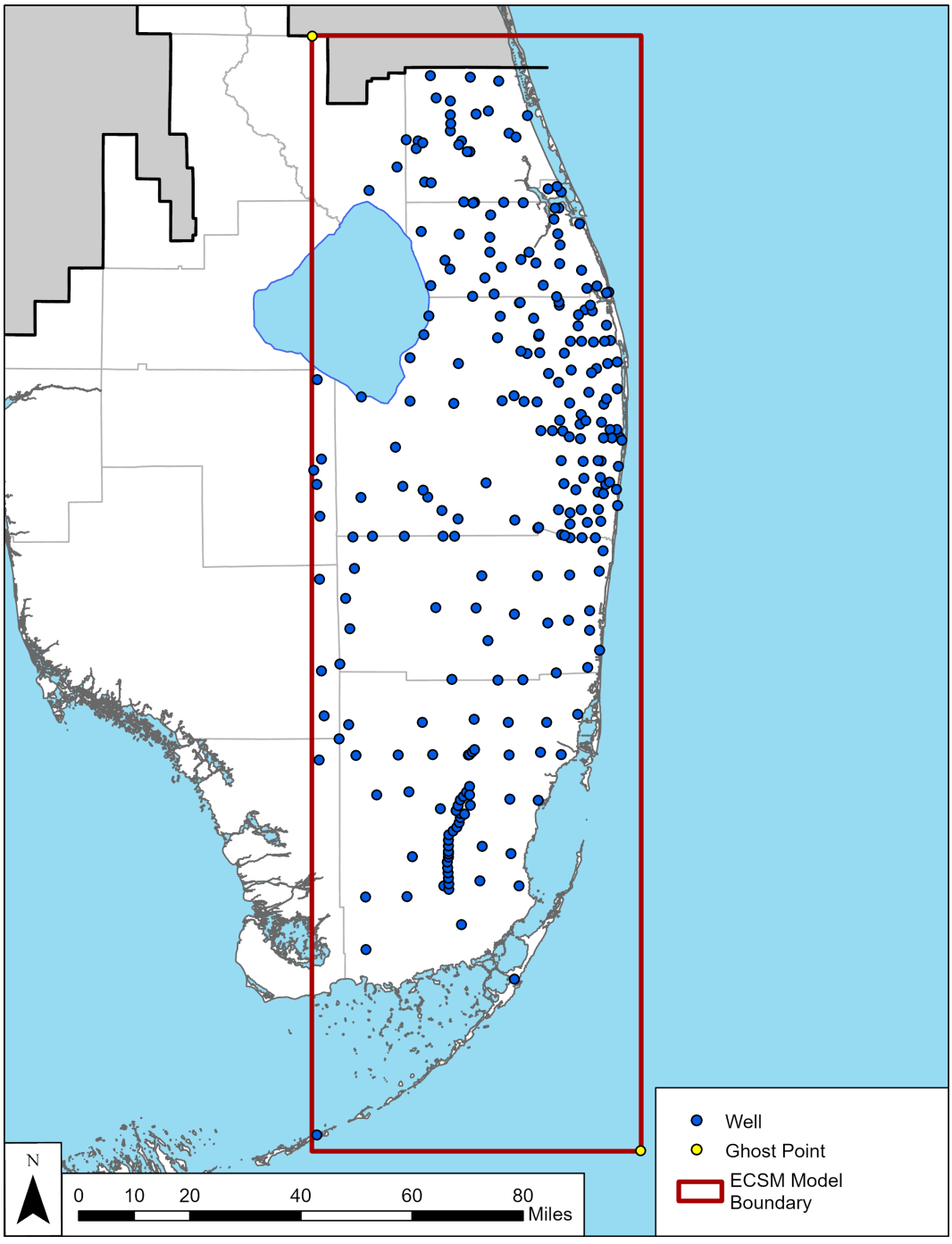

Figure 7. Locations of lithological control used in this study. Linear feature in southern Miami-Dade County is the L-31N Cut-Off Wall investigation.

5.1.1 Layer 1

Layer 1 encompasses the Holocene sediments, Q4, and Q5. The thickness of Layer 1 ranges from 3 feet in northwestern Miami-Dade County and western Collier County to 118 feet in eastern Palm Beach County (**Figure 8**). The top of Layer 1 (**Figure 9**) was assumed to be land surface. The elevation of the top of Layer 1 ranges from a maximum of 163 feet NAVD88 to a minimum of -4.4 feet NAVD88. Elevations are highest in Okeechobee County and southwest Indian River County. The region of lowest elevation is in southern Miami-Dade County.

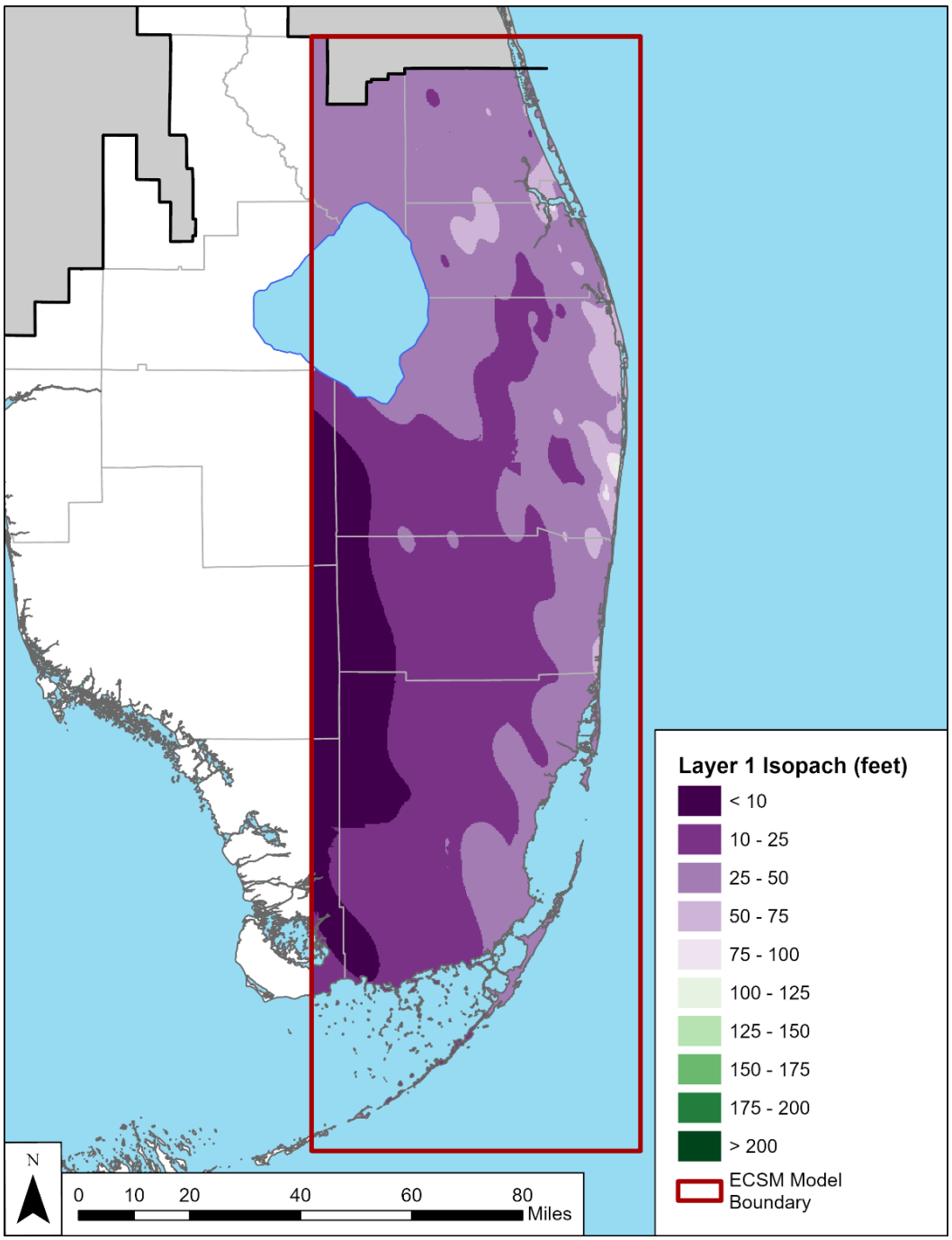

Figure 8. Layer 1 isopach map.

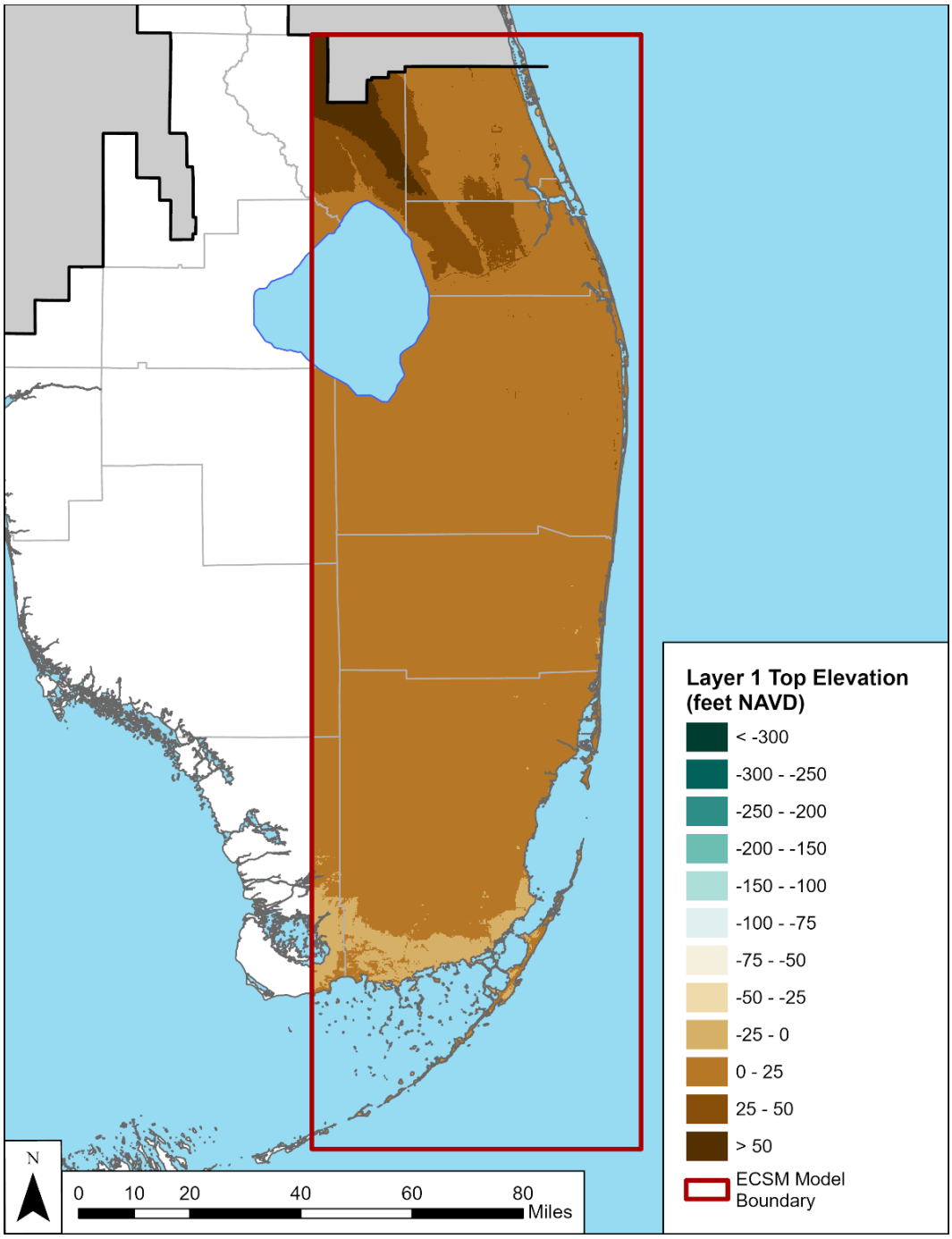

Figure 9. Elevation of the top of Layer 1.

5.1.2 Layer 2

Layer 2 encompasses Q2 and Q3. The thickness of Layer 2 ranges from 2 feet NAVD88 in eastern Hendry, Collier, and Monroe counties, and western Miami-Dade and Broward counties, to 110 feet in eastern Palm Beach County (**Figure 10**). The elevation of the top of Layer 2 ranges from a maximum of 117 feet NAVD88 to a minimum of -84.4 feet NAVD88 (**Figure 11**). The region of highest elevation is in Okeechobee County and southwest Indian River County. The region of lowest elevation is in eastern Palm Beach County.

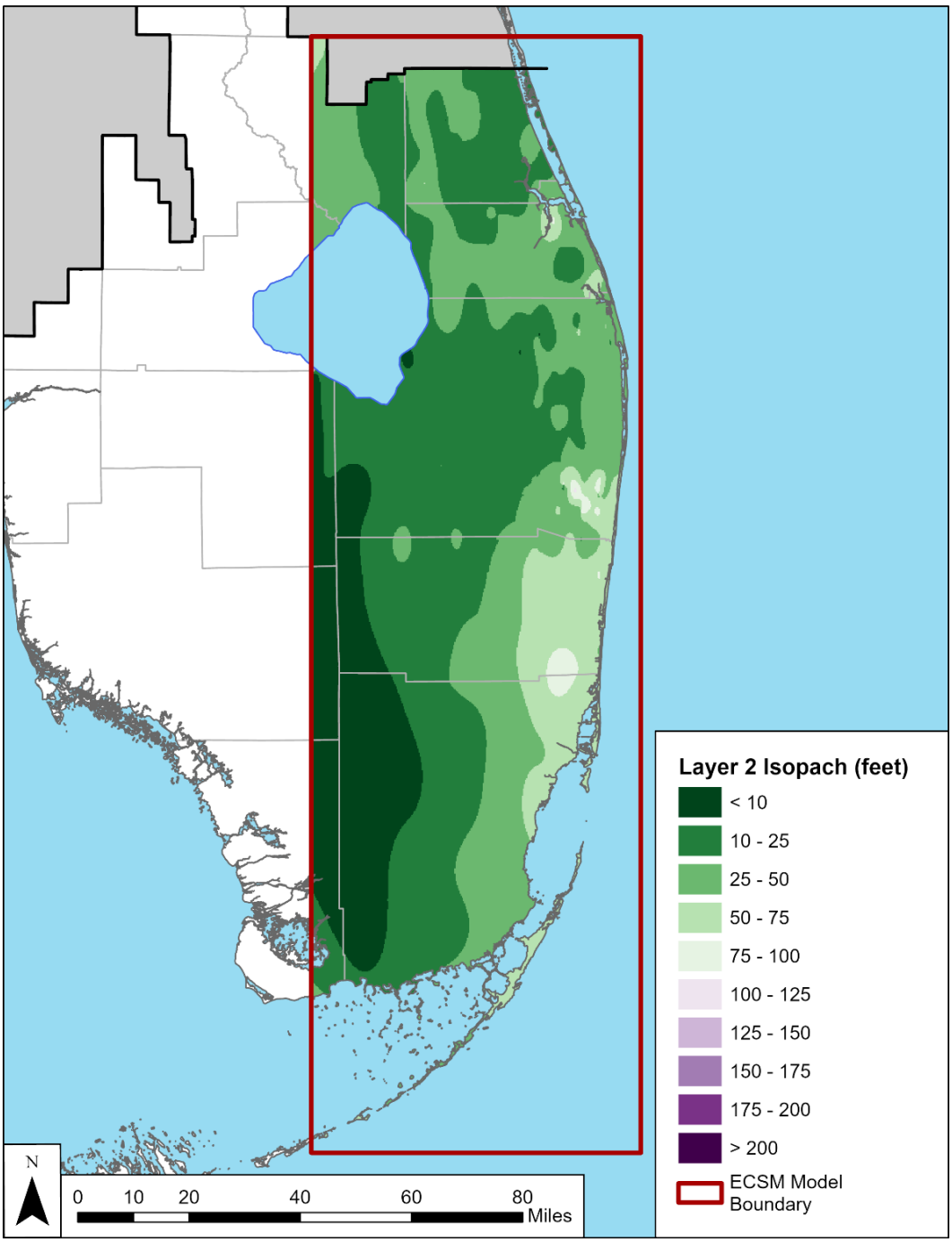

Figure 10. Layer 2 isopach map.

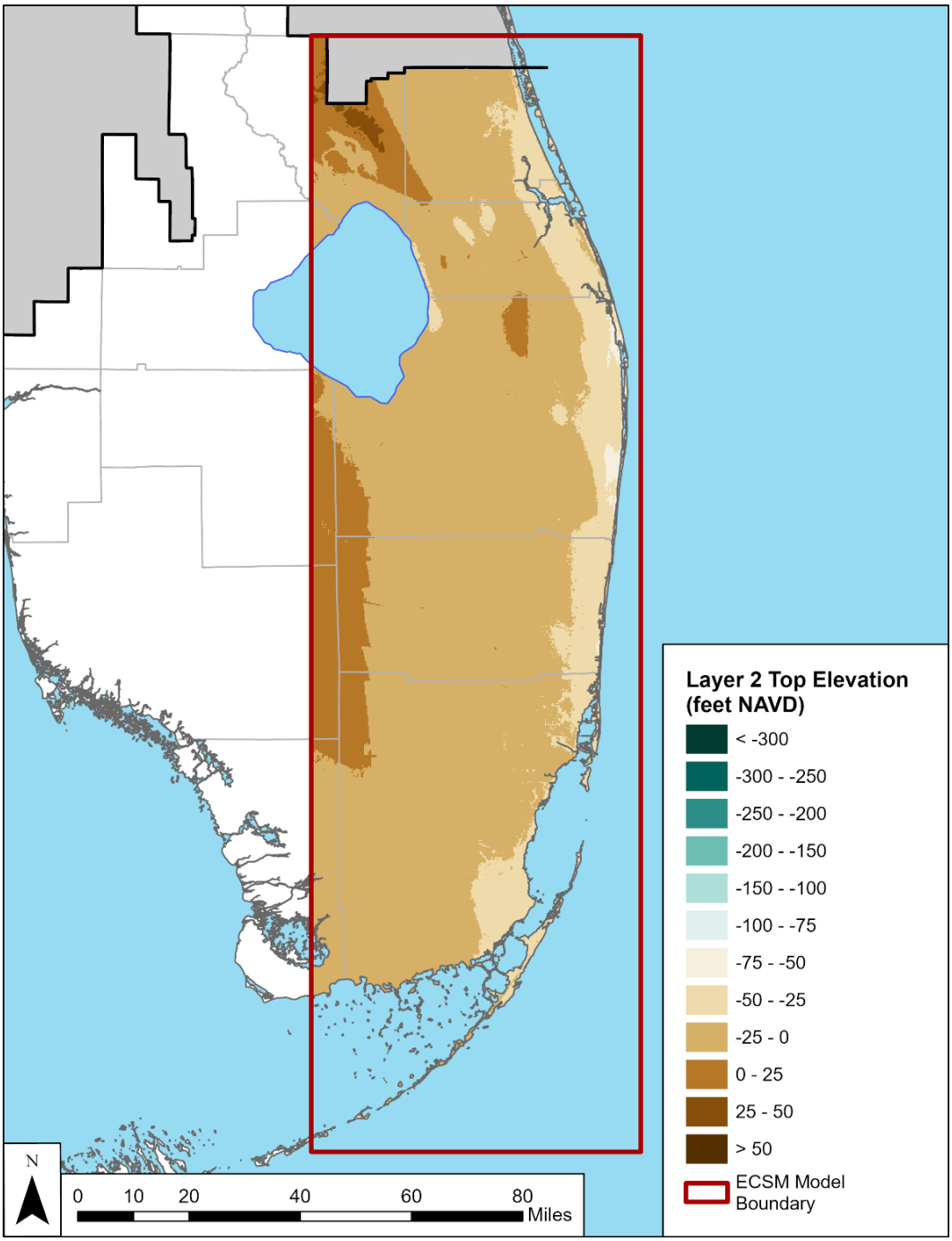

Figure 11. Elevation of the top of Layer 2.

5.1.3 Layer 3

Layer 3 encompasses Q1. The thickness of Layer 3 ranges from 1 foot in eastern Hendry, Collier, and Monroe counties, and western Miami-Dade and Broward counties to 49 feet in Martin County (**Figure 12**). The elevation of the top of Layer 3 ranges from a maximum of 85.3 feet NAVD88 to a minimum of -133.0 feet NAVD88 (**Figure 13**). The region of highest elevation is in eastern Collier and Hendry counties. The region of lowest elevation is in eastern Palm Beach and Broward counties.

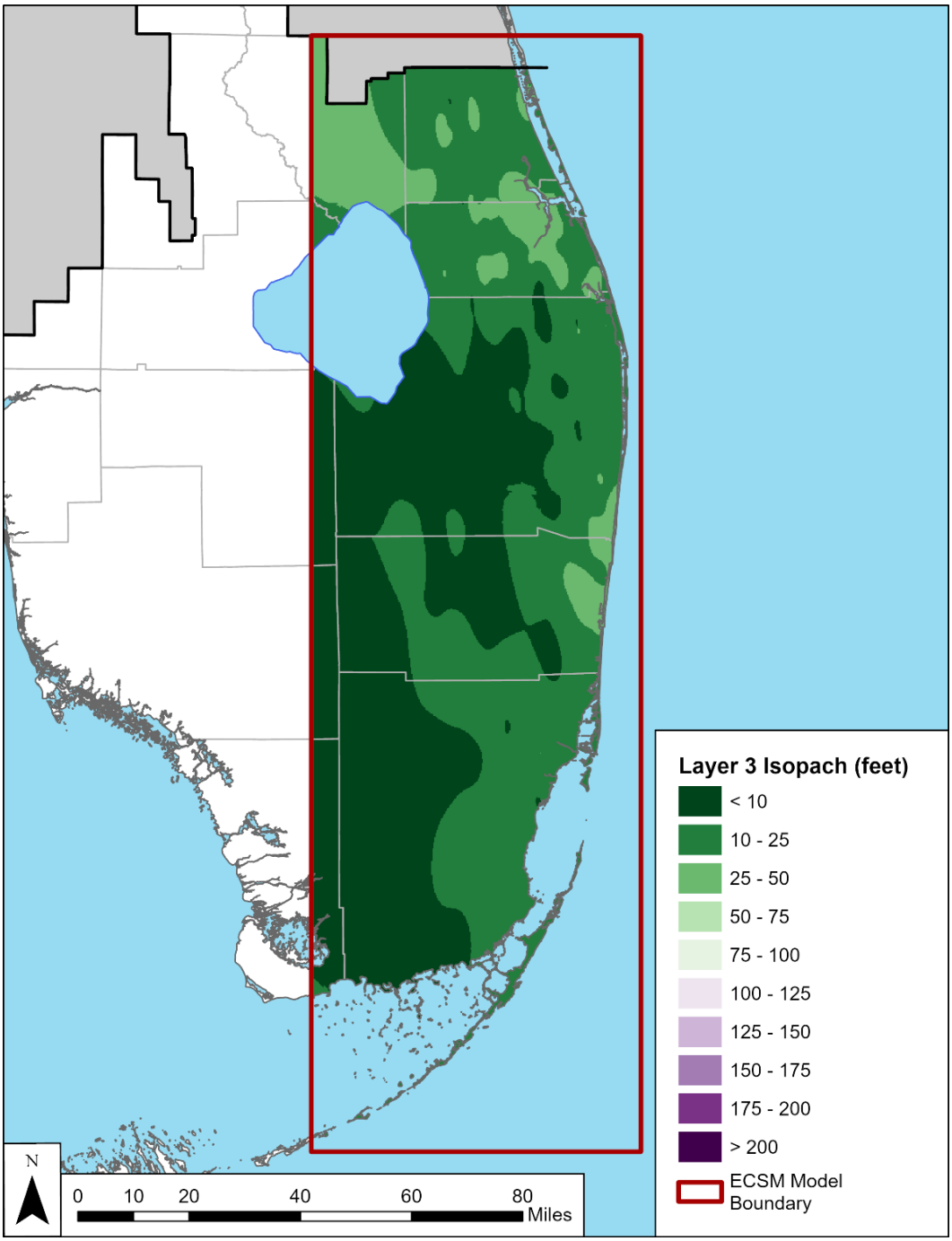

Figure 12. Layer 3 isopach map.

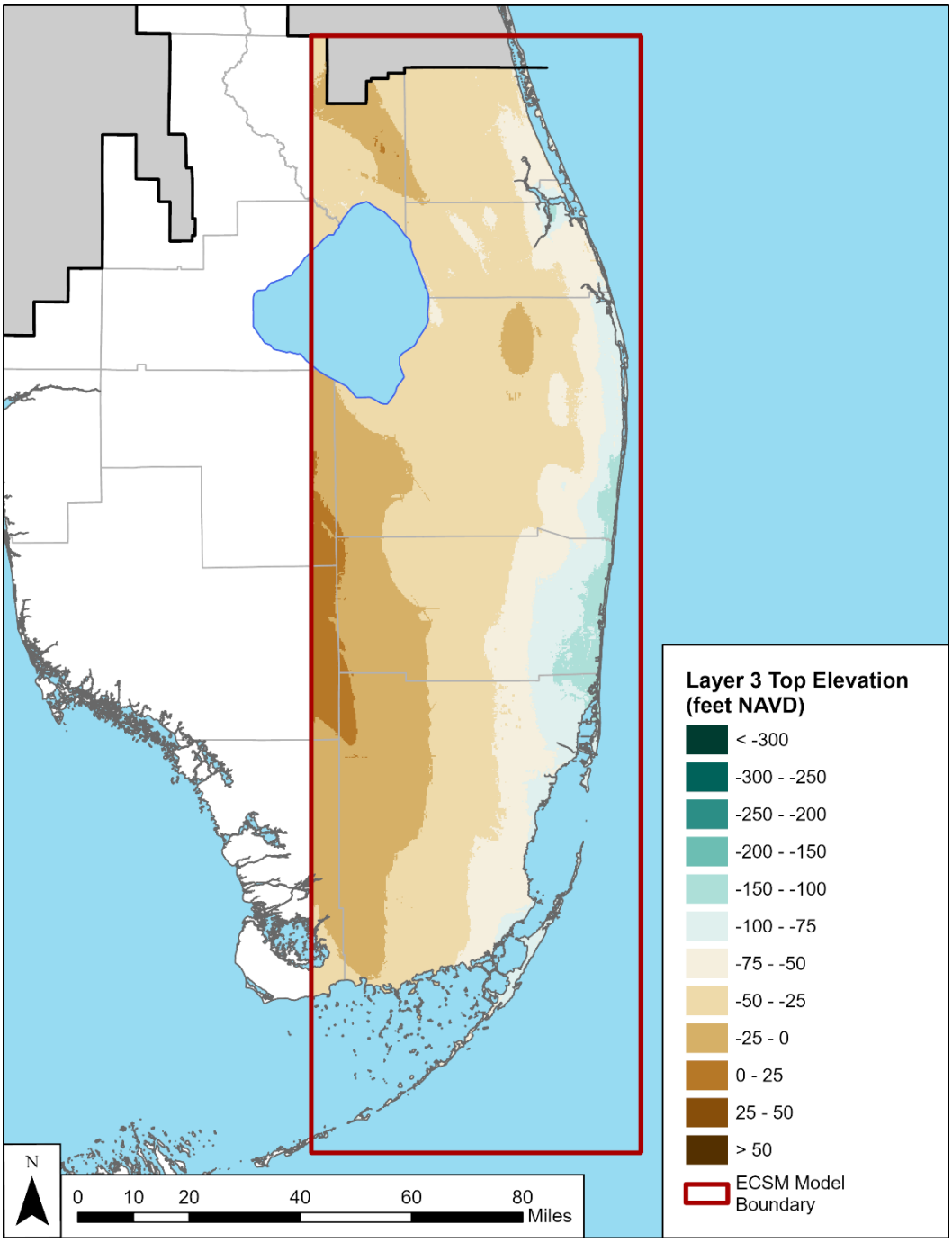

Figure 13. Elevation of the top of Layer 3.

5.1.4 Layer 4

Layer 4 encompasses the Pinecrest Sand Member of the Tamiami Formation. The thickness of Layer 4 ranges from 1 foot in eastern Collier and Monroe counties to 120 feet in Miami-Dade County (**Figure 14**). The elevation of the top of Layer 4 ranges from a maximum of 63.3 feet NAVD88 to a minimum of -159.6 feet NAVD88 (**Figure 15**). The region of highest elevation is in eastern Collier and Hendry counties. The region of lowest elevation is in eastern Palm Beach and Broward counties.

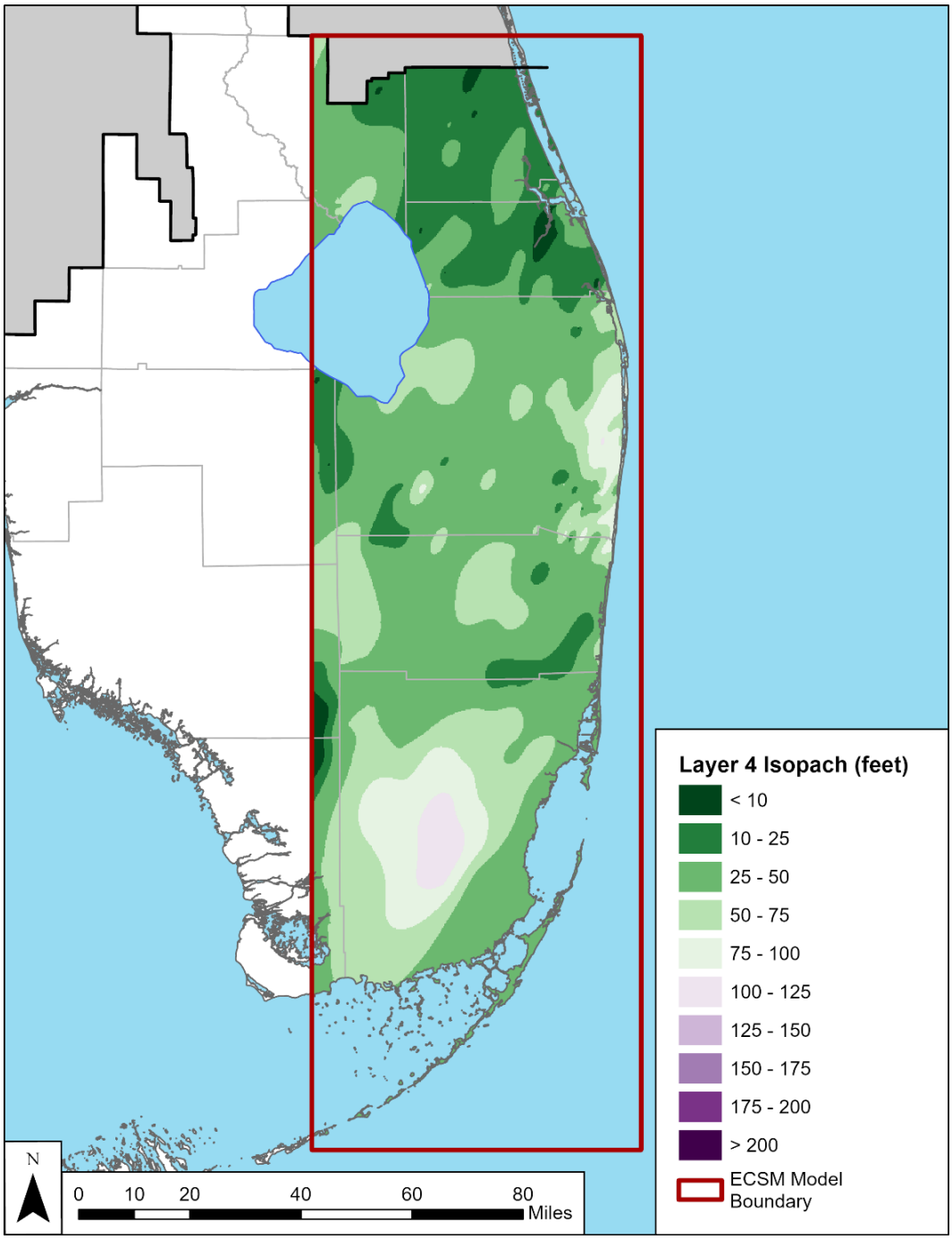

Figure 14. Layer 4 isopach map.

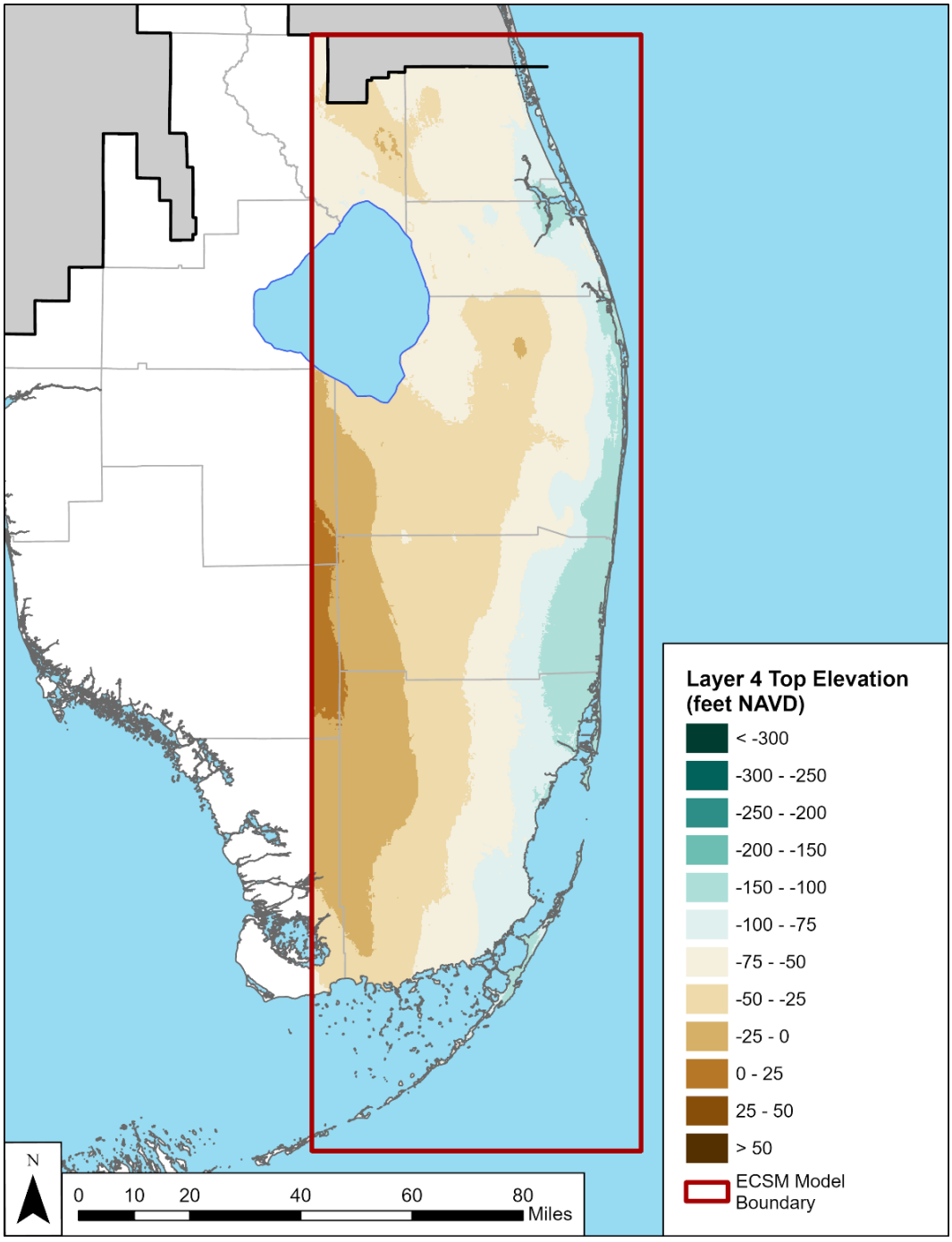

Figure 15. Elevation of the top of Layer 4.

5.1.5 Layer 5

Layer 5 encompasses the Ochopee Limestone Member of the Tamiami Formation. The thickness of Layer 5 ranges from 1 foot in Miami-Dade County to 208 feet in eastern Broward County (**Figure 16**). The elevation of the top of Layer 5 ranges from a maximum of 38.3 feet NAVD88 to a minimum of -243.6 feet NAVD88 (**Figure 17**). The region of highest elevation is in eastern Collier and Monroe counties. The region of lowest elevation is in eastern Palm Beach County. The elevation of the base of Layer 5 ranges from a maximum of 22.3 feet NAVD88 to a minimum of -380.1 feet NAVD88 (**Figure 18**). The region of highest elevation is in eastern Okeechobee County. The region of lowest elevation is in eastern Palm Beach and Broward counties.

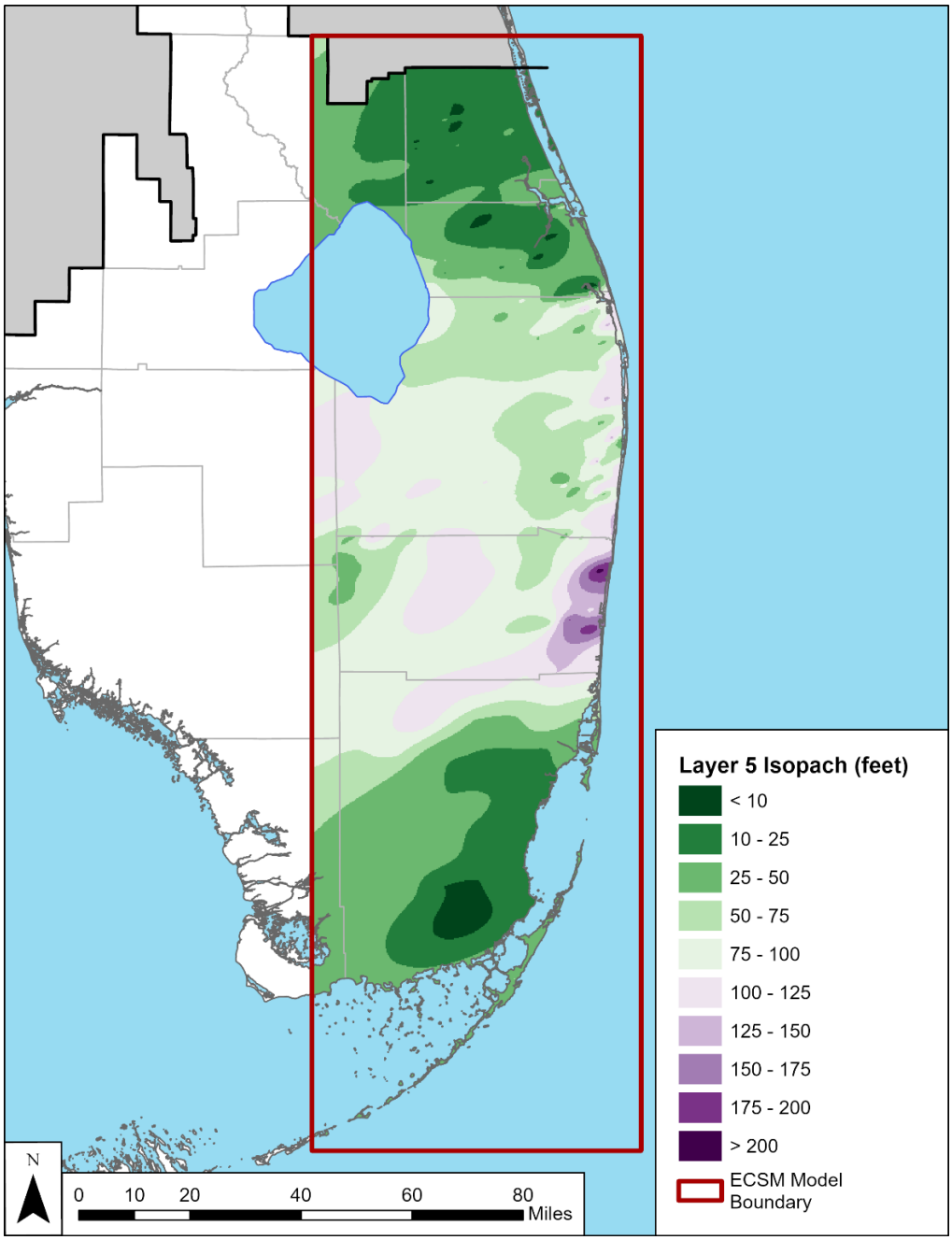

Figure 16. Layer 5 isopach map.

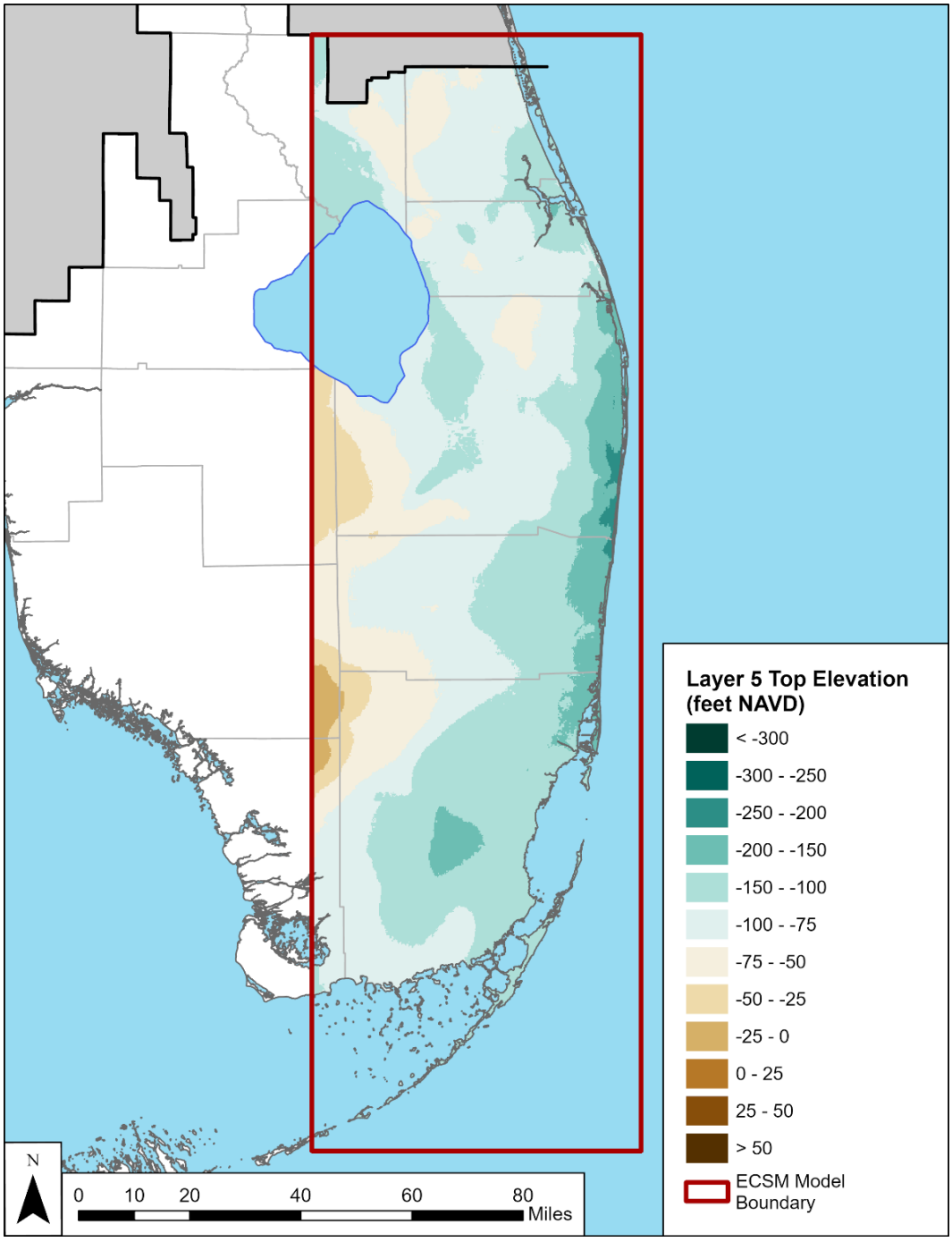

Figure 17. Elevation of the top of Layer 5.

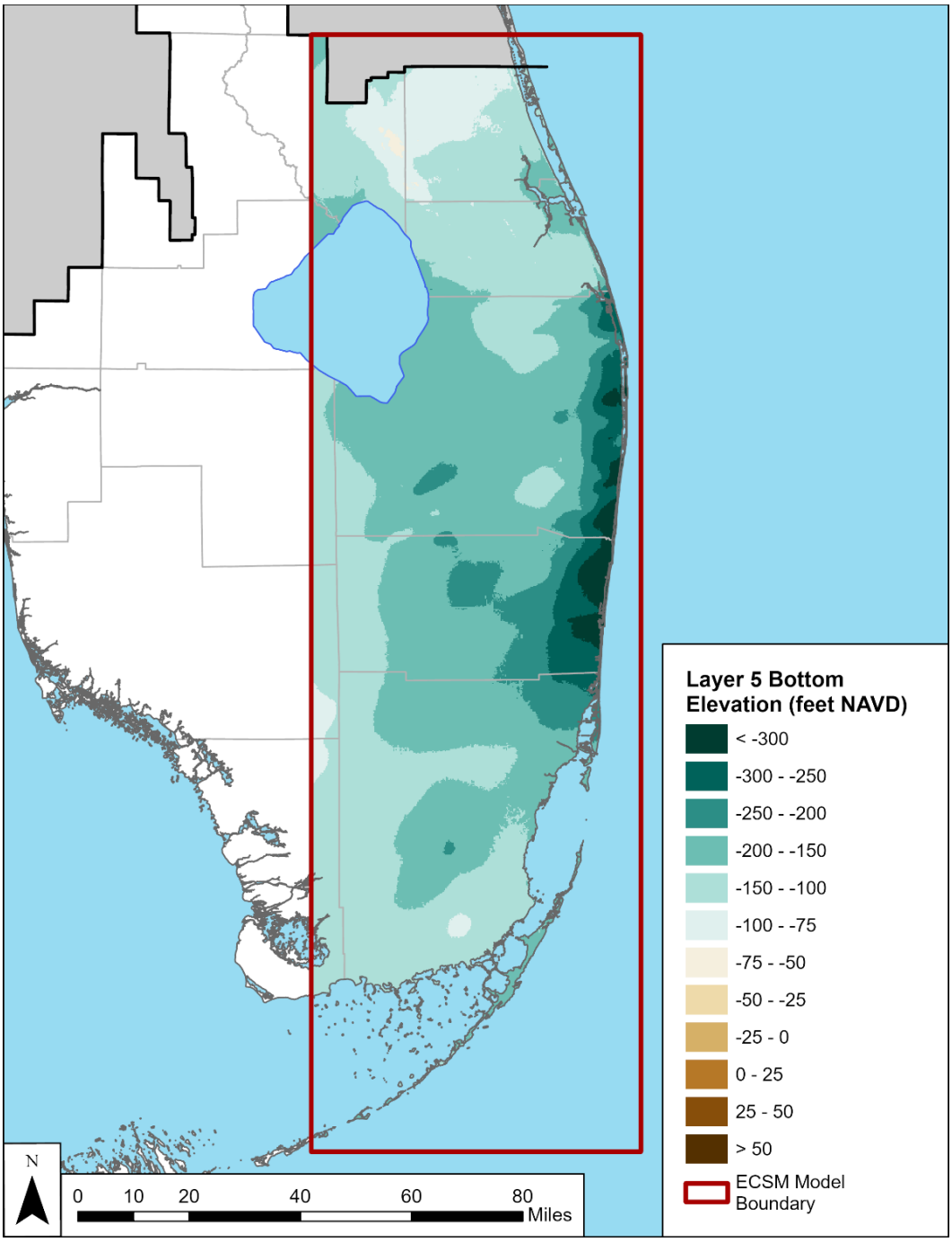

Figure 18. Elevation of the bottom of Layer 5.

5.2 Hydrogeologic Cross Sections

Eleven hydrogeologic cross sections were created using the software ParaView. **Figure 19** shows the hydrogeologic cross-sectional locations. The cross sections and cross-sectional locations are also included in **Appendix B**.

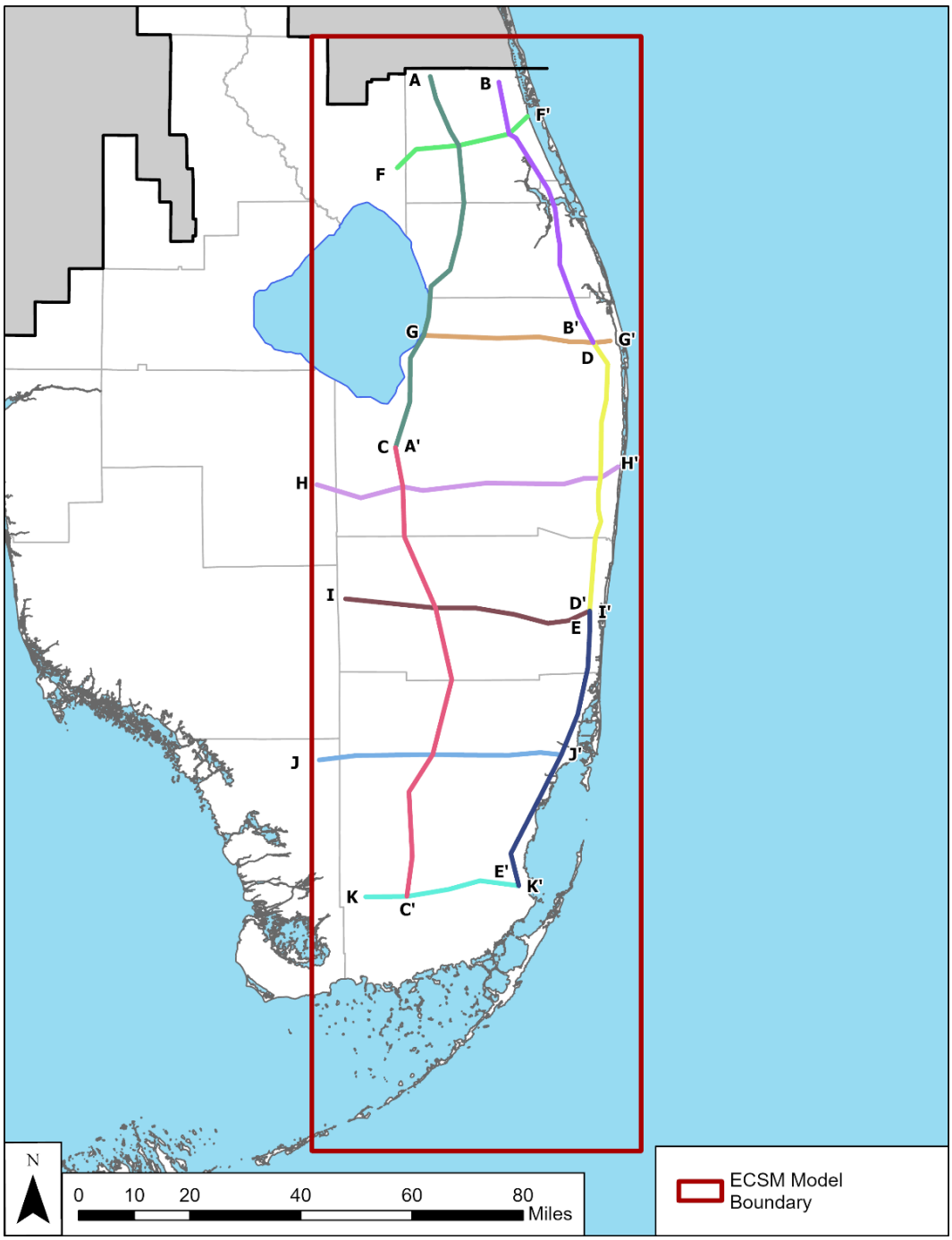

Figure 19. Hydrogeologic cross-sectional locations.

The cross section J-J' is shown in **Figure 20**. This cross section shows the general trend of the layers dipping east. Layer 5, the Ochopee Limestone, is thick to the west, which is the Gray Limestone aquifer. This layer gets thinner towards the coast as the aquifer disappears. Conversely, Layers 1 through 3 (Q1 through Q5) thicken towards the coast for the Biscayne aquifer.

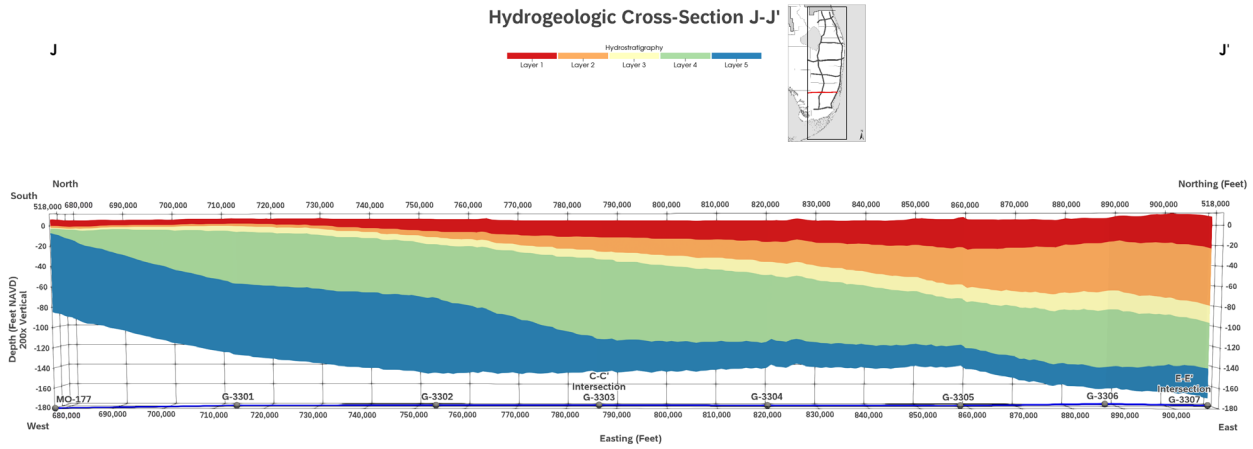

Figure 20. Cross section J-J'.

6 LIMITATIONS AND RECOMMENDATIONS

This project updates and refines the understanding of the hydrogeology of the SAS within the UEC and LEC planning areas for the purpose of supporting the ECSM. Technical uncertainties affecting the accuracy of the maps was predominantly caused by limited spatial coverage and variable data quality.

The primary limitation encountered during this study was the lack of wells and geologic data in lower population areas, due to well drilling and water supply investigations primarily occurring near populated areas. Areas of low population density included the stormwater treatment areas, water conservation areas, and Everglades National Park. These areas are undeveloped and often inundated, making access and construction of wells difficult. The wells located in these areas are often on the borders of the inundated areas or along cross-cutting roads or canals, with very few wells fully within these areas. This resulted in a much higher confidence of data along the coastlines and canals.

The accuracy of the elevations of the layers was hindered by the accuracy of the reviewed source data. The quality of the lithologic descriptions varied depending on sample collection methods, sample interval lengths, and/or the detail of individual descriptions. Reinterpretation of lithologic descriptions into Q units was not possible for some wells, such as descriptions with large sample interval lengths or which lacked information on fossils or organics. Wells where data were obtained from rock cores or split-spoon samples, optical borehole imaging, and geophysical data, resulted in layer boundary estimates that were more accurate.

A helpful follow-up to this report would be to use available geophysical logs to create a correlative framework across the project area and compare the reported lithostratigraphic and hydrogeologic unit boundaries to that framework. This would provide a means to evaluate the consistency of data interpretation for the formations and the hydrostratigraphic units based on these formations. This would also provide a valuable aid that could be used by local hydrogeologists for identifying Q units and formations, yielding more consistent data in the future.

7 LITERATURE CITED

Cooke, C.W. 1945. *Geology of Florida*. Geological Bulletin No. 29. State of Florida Department of Conservation, Florida Geological Survey, Tallahassee, FL. Prepared by the United States Geological Survey, Washington, DC. Published for the Florida Geological Survey. Florida Grower Press, Tampa, FL.

DuBar, J.R. 1962. *Neogene Biostratigraphy of the Charlotte Harbor Area in Southwestern Florida*. Geological Bulletin No. 43. State of Florida State Board of Conservation, Division of Geology, Florida Geological Survey, Tallahassee, FL.

ESRI. 2020. *ArcGIS Desktop*, version 10.8.1 [software]. Environmental Systems Research Institute, Redlands, CA. Available online at https://www.esri.com/en-us/arcgis/products/arcgis-desktop/resources/.

Geddes, E., E. Richardson, and A. Dodd. 2015. *Hydrogeologic Unit Mapping Update for the Lower West Coast Water Supply Planning Area*. Technical Publication WS-35. South Florida Water Management District, West Palm Beach, FL. August 2015.

GISGeography. 2022. *Kriging Interpolation – The Prediction Is Strong in This One.* Available online at https://gisgeography.com/kriging-interpolation-prediction/.

Golden Software. 2023. *Surfer*, Version 25.1.229 [software]. Golden Software, LLC., Golden, CO. Available online at https://www.goldensoftware.com/products/surfer/.

Hoffmeister, J.E. 1974. *Land from the Sea: The Geologic Story of South Florida*. University of Miami Press, Coral Gables, FL.

Hoffmeister, J.E., K.W. Stockman, and H.G. Multer. 1967. Miami Limestone of Florida and its recent Bahamian counterpart. *Geological Society of America Bulletin* 78(2): 175-190.

Hunter, M.E. and S.W. Wise, Jr. 1980. Possible Restriction and Redefinition of the Tamiami Formation of South Florida: Points for Further Discussion. Pages 41-44 in: P.J. Gleason (ed.), *Water, Oil, and the Geology of Collier, Lee, and Hendry Counties, Miami Geological Society Field Trip Guidebook*.

Kitanidis, P.K. 1997. *Introduction to Geostatistics: Applications in Hydrogeology*. Cambridge University Press, Cambridge, UK.

Kitware. 2023. *ParaView*, Version 5.11.2 [software]. Kitware Inc., Clifton Park, NY. Available online at https://www.paraview.org/.

Mansfield, W.C. 1939. *Notes on the Upper Tertiary and Pleistocene Mollusks of Peninsular Florida.* Geological Bulletin No. 18. State of Florida Department of Conservation. Published for the State Geological Survey, Tallahassee, FL.

Miller, J.A. 1986. *Hydrogeologic Framework of the Florida Aquifer System in Florida and in Parts of Georgia, Alabama, and South Carolina*. U.S. Geological Survey Professional Paper 1403-B. United States Geological Survey, Reston, VA.

Parker, G.G. and C.W. Cooke. 1944. *Late Cenozoic Geology of Southern Florida, with a Discussion of the Ground Water*. Geological Bulletin No. 27. State of Florida Department of Conservation. Published for the State Geological Survey, Tallahassee, FL.

Perkins, R.D. 1977. Depositional Framework of Pleistocene Rocks in South Florida. Pages 131-198 in: P. Enos and R.D. Perkins (eds.), *Quaternary Sedimentation in South Florida, Part II: The Geological Society of America Memoir 147*. The Geological Society of America, Boulder, CO.

Petuch, E.J. and C.E. Roberts. 2007. *The Geology of the Everglades and Adjacent Areas*. CRC Press, Boca Raton, FL.

Reese, R.S. and K.J. Cunningham. 2000. *Hydrogeology of the Gray Limestone Aquifer in Southern Florida*. Water-Resources Investigations Report 99-4213. Prepared in cooperation with the South Florida Water Management District, West Palm Beach, FL. United States Geological Survey, Tallahassee, FL.

Reese, R.S. and M.A. Wacker. 2007. *Hydrostratigraphic Framework and Selection and Correlation of Geophysical Log Markers in the Surficial Aquifer System, Palm Beach County, Florida*. Scientific Investigations Map 2971. Prepared in cooperation with the South Florida Water Management District, West Palm Beach, FL. United States Geological Survey, Reston, VA.

Reese, R.S., and M.A. Wacker. 2009. *Hydrogeologic and Hydraulic Characterization of the Surficial Aquifer System, and Origin of High Salinity Groundwater, Palm Beach County, Florida*. Scientific Investigations Report 2009-5113. Prepared in cooperation with the South Florida Water Management District, West Palm Beach, FL. United States Geological Survey, Reston, VA.

Scott, T.M. 1988. *The Lithostratigraphy of the Hawthorn Group (Miocene) of Florida*. Bulletin No. 59. Florida Geological Survey, Tallahassee, FL.

Scott, T.M. 2001. *Text to Accompany the Geologic Map of Florida*. Open-File Report 80. Florida Geological Survey, Tallahassee, FL.

Wacker, M.A., K.J. Cunningham, and J.H. Williams. 2014. *Geologic and Hydrogeologic Frameworks of the Biscayne Aquifer in Central Miami-Dade County, Florida*. Scientific Investigations Report 2014-5138. Prepared in cooperation with the Miami-Dade County Water and Sewer Department, Miami, FL. United States Geological Survey, Reston, VA.

Zumbro, J., S. Coonts, and A. Bouchier. 2023. *Hydrostratigraphy and Aquifer Hydraulic Properties Update for the Surficial and Intermediate Aquifer Systems, Lower West Coast Planning Area*. Technical Publication WS-62. South Florida Water Management District, West Palm Beach, FL. July 2023.

APPENDICES

APPENDIX A:
DATA USED FOR HYDROSTRATIGRAPHIC SURFACE CREATION

Well	Row	Column	X	Y	Land Surface Elevation (ft NAVD 88)	Layer 1 Thickness (ft)	Layer 2 Thickness (ft)	Layer 3 Thickness (ft)	Layer 4 Thickness (ft)	Layer 5 Thickness (ft)
C-1134	647	12	683275	556569	7.2	5	2	1	1	78
C-1138	604	10	680532	599237	9.1	4	2	1	18	88
C-1169	517	8	678822	686296	13.0	7	2	1	70	64
FPL-MA	214	127	798008	989257	30.3	20	40	20	40	51
G-2311	575	168	838897	627922	7.7	19	49	7	30	79
G-2312	514	162	833169	689687	9.7	13	23	3	66	116
G-2313	476	88	759409	726901	10.1	30	30	15	20	61
G-2314	477	40	710644	726204	12.0	8	6	3	70	46
G-2315	476	125	796256	727007	9.6	24	16	8	63	123
G-2316	612	134	804461	591141	6.7	13	27	19	33	104
G-2317	613	177	848367	590305	2.9	11	40	24	16	120
G-2318	613	201	872007	590619	3.6	20	53	16	20	94
G-2319	544	157	827646	658972	6.3	13	23	10	64	96
G-2320	544	118	789098	659137	7.5	12	20	10	38	122
G-2321	550	193	864037	652975	7.2	19	44	10	70	80
G-2322	559	225	895802	644559	6.5	34	60	10	50	64
G-2323	478	246	916911	725559	14.7	38	77	20	10	114
G-2325	478	270	940842	725713	11.5	73	40	40	25	120
G-2327	606	233	903733	597353	5.6	24	89	10	23	126
G-2328	601	263	933818	602484	9.2	46	74	14	30	120
G-2329	535	32	703430	667841	11.7	8	6	3	70	46
G-2338	564	37	707656	639375	9.7	8	6	3	70	46
G-2340	507	41	712048	696524	10.4	8	6	3	70	46
G-2341	514	215	885896	689536	9.0	19	67	20	13	60
G-2342	513	246	916674	690218	10.7	36	67	30	43	120
G-2344	509	273	944426	693930	17.8	49	77	20	38	208
G-2345	556	245	915571	647097	8.1	29	67	17	30	178
G-2346	598	27	698025	605645	8.4	3	2	1	52	77
G-2347	566	265	935596	637733	5.0	37	67	23	20	189
G-2610	584	274	944841	618913	0.4	62	48	20	70	100
G-2916	490	277	948411	713354	14.9	42	60	30	85	110
G-3295	655	36	706577	548109	6.5	3	2	1	52	77
G-3296	653	105	776372	550266	6.5	15	14	10	38	118
G-3297	650	155	825877	553259	5.4	19	22	15	62	52
G-3298	653	187	858140	550066	5.7	26	32	10	70	40
G-3299	653	224	894685	550152	6.2	35	59	13	43	70
G-3300	645	253	924149	557796	8.3	37	61	20	50	53
G-3301	685	42	713285	518740	7.6	5	3	9	53	71
G-3302	684	82	753419	519316	6.7	14	6	8	53	78
G-3303	684	115	786330	519705	5.5	17	14	6	82	31
G-3304	684	149	820250	519215	4.9	23	20	6	70	26
G-3305	684	188	858924	519075	8.1	33	38	12	45	21
G-3306	682	218	888717	521648	8.1	21	47	26	60	21
G-3307	684	238	908568	519538	8.1	32	57	17	45	31
G-3308	722	62	733190	481418	4.7	7	5	3	92	46
G-3309	719	93	763745	484209	5.5	10	6	6	78	35
G-3310	735	123	793624	468140	5.1	22	18	10	114	26
G-3311	732	151	821895	471469	6.4	19	22	14	82	33
G-3312	726	189	859577	477282	6.9	22	40	20	60	21
G-3313	727	216	886671	476306	11.0	36	70	10	40	21
G-3314	777	131	801452	426169	5.2	20	24	15	120	36
G-3315	771	162	833219	432444	11.7	38	32	16	80	11
G-3316	778	190	860550	425597	5.1	26	36	16	40	21
G-3317	819	52	722540	384387	1.5	17	4	7	58	38
G-3318	819	91	761789	384767	3.4	23	19	4	94	31
G-3319	809	126	796788	394758	4.2	15	24	15	100	11
G-3320	804	160	831334	399727	2.0	32	40	24	30	11
G-3321	808	197	868211	394943	0.6	32	33	23	40	21
G-3322	869	52	722982	334520	-0.3	7	4	6	64	31
G-3323	845	143	813698	357968	0.6	20	18	7	30	1
G-3394	781	96	766920	422737	3.9	16	20	5	95	26
G-563	547	265	935565	656412	5.3	37	73	44	27	120
HE-1110	457	8	679154	746065	14.8	7	2	1	30	114
HE-1116	413	2	673316	789880	15.8	5	4	2	35	107
HY-202	328	6	676635	875701	17.1	15	10	10	10	80
HY209	403	16	680486	800384	13.7	7	13	10	10	116
HY-312	427	5	676229	776453	12.2	10	10	10	30	90
L31CW-B02	812	131	801538	391498	4.9	21	18	17	80	14
L31CW-B04	806	131	801492	396821	3.9	21	20	15	89	13
L31CW-B06	801	131	801456	402066	4.1	21	17	23	88	15
L31CW-B08	796	130	800883	407121	4.5	21	21	13	100	17

Well	Row	Column	X	Y	Land Surface Elevation (ft NAVD 88)	Layer 1 Thickness (ft)	Layer 2 Thickness (ft)	Layer 3 Thickness (ft)	Layer 4 Thickness (ft)	Layer 5 Thickness (ft)
L31CW-B10	791	130	800447	412206	4.4	26	15	15	104	21
L31CW-B12	786	129	800351	417503	4.9	22	15	19	110	25
L31CW-B14	781	130	801297	422346	4.8	23	13	24	113	31
L31CW-B15	778	130	801309	424981	5.3	26	15	17	119	35
L31CW-B16	776	130	801270	427681	4.9	26	16	19	117	36
L31CW-B18	770	130	801179	432949	4.9	26	20	10	120	33
L31CW-B20	765	130	801099	438231	5.2	27	20	9	118	32
L31CW-B22	760	131	801786	443312	5.5	22	20	14	115	30
L31CW-B24	756	135	805532	446946	5.6	22	23	11	113	28
L31CW-B26	753	138	809337	450596	5.8	23	21	12	109	27
L31CW-B28	748	141	811612	454876	6.0	23	20	18	99	28
L31CW-B30	744	142	812742	459754	6.0	21	23	12	100	28
L31CW-B34	740	142	812590	463622	6.1	21	21	14	97	29
L31CW-B36	737	138	808521	466315	5.8	22	18	16	98	30
L31CW-B39	732	139	810345	471225	5.9	23	21	12	93	30
L31CW-B42	727	142	812736	476703	5.7	21	17	18	87	31
L31CW-B44	724	144	815422	479676	5.8	18	25	13	84	31
L31CW-B47	719	148	818570	483941	5.8	21	19	16	80	30
L31CW-B50	714	150	821238	489189	6.3	20	21	20	73	28
L31CW-B52	684	150	821280	519428	5.0	21	21	19	62	27
L31CW-B53	681	153	823776	522004	4.5	20	23	18	62	28
L31CW-B54	679	155	826199	524437	5.0	22	22	12	67	29
L31CW-B55	722	151	821512	481471	6.5	21	22	13	80	30
LARGO	897	193	863972	306175	1.4	32	70	22	30	51
LCW31-B32	740	146	816614	463239	6.5	22	22	22	83	30
M-1043	149	238	908486	1054275	22.0	50	40	20	50	45
M-1053	179	255	925977	1024001	3.2	30	40	20	50	45
M-1091	164	235	906280	1039023	11.6	30	40	20	50	55
M-1096	238	220	891270	965527	20.7	24	30	10	40	47
M-1361	238	114	784621	965032	16.3	41	23	12	53	88
M-1367	246	174	844598	957205	24.3	26	28	14	34	66
M-656	164	232	902687	1038911	11.1	94	74	37	10	21
Marathon	1045	5	676069	158371	0.5	32	70	22	30	51
MO-177	689	7	678364	514569	6.3	6	2	1	1	79
MO-178	669	26	697271	534673	6.6	6	2	1	40	81
NWCORN	1	1	671893	1202335	67.1	50	60	35	60	60
OKF-106	148	55	725845	1055706	24.1	30	30	30	60	20
OKS-82	126	82	752584	1077753	53.9	38	20	30	30	35
PB-1065	317	271	942201	886475	13.2	67	33	17	72	62
PB-1082	290	284	955152	913226	11.3	61	24	12	42	62
PB-1083	291	279	949722	912480	15.5	56	39	19	40	47
PB-1084	291	257	927800	912330	15.7	40	32	16	36	66
PB-1085	291	246	917383	912263	17.5	38	30	15	33	72
PB-1086	292	268	939039	911496	17.1	47	37	19	43	55
PB-1087	318	247	918009	884801	17.7	37	25	12	42	75
PB-1089	340	264	934738	863643	16.3	38	28	14	41	96
PB-1090	368	276	946635	835512	17.8	48	35	18	92	43
PB-1091	370	255	926227	833658	17.1	52	21	10	56	62
PB-1092	376	239	909840	826891	16.5	30	22	11	52	67
PB-1093	376	229	899944	827236	14.1	27	22	11	35	76
PB-1094	376	218	889141	827477	13.6	33	20	10	38	65
PB-1095	405	275	946257	798451	16.2	56	33	17	89	56
PB-1096	405	259	929452	798338	18.8	36	31	16	61	65
PB-1097	404	238	908507	798908	15.0	21	26	13	33	61
PB-1098	302	241	911564	900917	19.1	35	28	14	38	62
PB-1099	277	254	924625	926750	15.2	35	28	14	43	51
PB-1100	475	238	908706	728436	13.9	34	27	13	55	66
PB-1101	451	273	943753	752692	15.3	35	85	20	40	120
PB-1102	432	251	922175	771331	19.1	49	34	17	55	61
PB-1103	451	257	927568	752383	18.4	30	90	20	20	60
PB-1104	434	273	943643	768847	16.8	35	85	20	40	120
PB-1105	478	257	928286	725630	14.4	46	24	12	91	68
PB-1106	461	194	864510	742331	10.7	35	26	13	41	86
PB-1107	426	240	910970	776994	14.0	24	81	24	11	29
PB-1108	451	235	906017	752250	13.6	37	58	10	19	51
PB-1109	286	216	887101	916930	21.0	31	31	16	34	49
PB-1144	244	283	953620	959050	6.8	63	45	22	59	145
PB-1166	269	211	882296	934069	23.4	32	25	12	35	62
PB-1168	454	246	917038	749288	17.2	32	29	14	66	89
PB-1173	366	236	906887	837046	15.3	61	35	18	58	96
PB-1176	330	235	906020	873419	17.4	46	39	20	28	81

Well	Row	Column	X	Y	Land Surface Elevation (ft NAVD 88)	Layer 1 Thickness (ft)	Layer 2 Thickness (ft)	Layer 3 Thickness (ft)	Layer 4 Thickness (ft)	Layer 5 Thickness (ft)
PB-1184	307	94	764971	896740	9.5	31	21	11	38	81
PB-1192	404	272	943436	798937	17.6	60	35	17	97	133
PB-1195	410	292	962649	793501	13.6	118	43	21	86	117
PB-1197	261	260	931132	942243	15.7	58	31	15	46	128
PB-1428	469	215	886289	734570	10.3	16	50	14	53	60
PB-1544	361	257	927498	842619	16.9	42	26	13	55	81
PB-1546	257	236	906485	946427	18.5	18	50	25	10	60
PB-1550	284	217	887451	918850	20.4	15	10	5	50	95
PB-1558	303	205	876045	900613	20.4	18	16	10	47	68
PB-1605	436	278	948670	767578	13.9	83	47	23	82	41
PB-1613	267	179	850418	936028	22.8	24	31	15	33	47
PB-1693	336	291	961831	867127	15.5	51	45	22	82	114
PB-1695	351	278	948922	852551	16.0	50	45	22	94	112
PB-1702	427	280	950679	776470	13.2	80	46	23	91	121
PB-1703	439	47	718231	763974	11.3	6	4	2	30	101
PB-1704	452	124	794993	751335	8.9	16	26	8	23	85
PB-1761	468	216	887047	735463	10.0	22	25	13	53	88
PB-1769	382	293	963909	821069	17.6	67	47	23	92	22
PB-1775	476	241	911588	727632	14.0	41	17	10	64	80
PB-1781	343	193	863794	860661	21.5	29	24	12	56	80
PB-1782	321	266	937346	882542	18.5	42	27	14	40	88
PB-1783	321	226	896557	881831	19.5	43	27	14	32	75
PB-1784	447	291	962201	756228	2.4	68	67	34	89	119
PB-1785	439	111	781643	764246	9.9	13	18	10	42	87
PB-1787	429	87	757930	774450	8.9	15	15	10	25	89
PB-1788	460	139	810299	743310	10.9	14	23	12	33	81
PB-1804	425	166	837115	777941	12.0	22	19	10	56	102
PB-1805	392	80	750958	811645	9.4	13	17	10	44	97
PB-1806	350	246	916460	853515	17.9	28	25	13	52	71
PB-1807	383	256	926566	819832	19.4	38	21	10	58	76
PB-600	375	291	961481	828347	17.2	57	47	24	78	114
PB-640	254	235	906254	949452	18.5	25	33	16	36	87
PB-649	254	198	868730	948941	23.5	22	28	14	38	60
PB-650	248	153	824087	954996	22.9	34	21	10	35	68
PB-651	267	112	782520	936370	14.5	40	23	12	43	86
PB-652A	311	291	961555	892468	11.8	65	35	17	69	113
PB-653	312	282	952681	891195	11.0	67	33	17	72	114
PB-657	367	261	931651	836724	17.2	53	36	18	81	81
PB-658	463	262	933378	740102	16.6	42	48	24	72	112
PB-665	465	246	917013	738585	16.4	41	27	13	77	90
PB-666	462	275	946194	741401	10.9	39	61	31	87	121
PB-667	346	280	951379	857458	13.6	47	49	25	100	130
PB-668	375	284	954672	828400	11.6	51	39	20	65	96
PB-669	383	286	956545	820436	9.5	38	36	18	96	138
PB-670	383	278	948735	820583	15.4	62	39	19	103	87
PB-672	382	245	916137	821377	18.9	27	27	13	56	64
PB-673	421	259	929919	782287	18.9	25	41	20	53	90
PB-674	421	275	945728	782696	15.5	36	45	22	43	90
PB-675	425	284	954484	778313	14.0	69	43	21	88	109
PB-676	347	181	852426	855865	7.6	19	19	10	39	80
PB-677	348	202	873293	855060	14.5	29	21	11	58	74
PB-678	349	215	885541	854620	16.6	33	27	14	49	63
PB-679	302	217	888002	901486	19.6	26	29	14	31	51
PB-681	245	280	951386	958439	11.8	46	37	19	47	92
PB-690	432	290	960899	771608	10.6	40	77	28	30	100
PB-712	262	267	938022	940976	13.9	57	27	14	53	50
PB-747	257	265	936330	946546	12.1	54	37	19	42	99
PB-830	288	177	847990	915653	21.1	27	23	12	30	59
PB-833	276	280	951424	927740	11.1	58	53	26	62	130
PB-834B	385	295	965932	818125	8.7	41	47	24	69	20
PB-836	350	136	806539	853251	9.6	35	21	11	51	83
PB-837	312	140	810843	891029	9.2	28	23	11	65	74
PB-838	285	107	777775	918383	10.5	30	21	11	42	90
PB-839	348	94	764716	855443	13.7	28	21	11	43	84
PB-840	432	106	777115	770867	9.9	20	20	10	90	120
PB-841	476	136	807264	727246	11.4	30	29	15	35	112
PB-842	476	58	728950	726909	11.3	12	22	11	15	131
PB-843	344	48	718452	859488	14.2	24	24	12	39	112
PB-880	266	254	925013	937592	15.3	29	24	12	29	73
SECORN	1060	313	983899	143325	-2.0	40	20	10	10	20
SR76_PWM31	175	231	901536	1028163	10.4	50	80	40	10	21

Well	Row	Column	X	Y	Land Surface Elevation (ft NAVD 88)	Layer 1 Thickness (ft)	Layer 2 Thickness (ft)	Layer 3 Thickness (ft)	Layer 4 Thickness (ft)	Layer 5 Thickness (ft)
W-12668	213	199	870234	989843	26.2	20	50	20	40	51
W-16193	300	199	870324	902802	20.3	14	10	5	50	65
W-16283	144	233	904352	1059311	16.1	45	35	25	15	45
W-16284	223	132	802811	980705	23.0	33	49	28	10	25
W-16287	189	234	905369	1014565	15.6	40	22	23	50	15
W-16289	101	143	813832	1102785	23.0	50	25	25	12	16
W-16290	159	155	826249	1044369	27.5	55	25	25	17	20
W-16371	76	132	803194	1127384	22.2	35	38	14	12	10
W-16372	63	132	803236	1140613	21.1	39	36	10	14	11
W-16373	101	102	772540	1102746	28.3	31	35	17	11	10
W-16374	108	100	770487	1095369	29.6	51	12	19	19	10
W-16375	76	206	876544	1126809	15.5	55	18	31	18	20
W-16376	75	156	827429	1128288	20.0	33	36	32	10	14
W-16377	100	90	761087	1103725	31.3	35	22	18	27	14
W-16383	104	140	811141	1099038	22.6	44	13	17	34	27
W-16384	91	132	803250	1112036	22.6	25	25	32	23	10
W-16385	84	132	803315	1118903	22.3	30	30	14	28	11
W-16397	224	257	927988	979686	11.3	55	15	17	13	38
W-16398	217	213	884268	986690	21.8	35	50	15	11	13
W-16400	171	170	841382	1032317	27.7	65	27	28	22	10
W-16460	199	236	907219	1003991	11.5	52	28	17	23	20
W-16525	93	188	858877	1109954	17.6	37	39	13	12	21
W-16530	97	195	865478	1106150	10.9	40	24	16	41	19
W-16543	111	151	821556	1092299	22.3	40	20	20	20	20
W-16931	140	108	778518	1063786	30.5	34	51	30	14	11
W-16932	39	113	783974	1164682	21.8	33	35	12	15	11
W-16933	103	106	776964	1100740	27.6	21	35	17	17	25
W-16935	159	145	816046	1044529	25.8	44	25	10	26	35
W-16936	72	168	839218	1131066	19.8	53	13	14	20	25
W-16957	140	114	784838	1062897	23.0	30	30	30	20	10
W-16963	146	225	896150	1057142	15.9	60	30	20	30	50
W-16964	44	178	849174	1159388	18.5	33	25	22	17	15
W-17023	60	119	789445	1143595	21.3	20	20	20	20	20
W-17025	40	151	822150	1163081	23.3	40	22	25	10	23
W-17037	254	199	869541	949045	23.4	13	29	13	15	84
W-17136	111	148	819193	1092406	22.9	40	10	30	20	30
W-50067	241	262	933003	962635	7.5	40	33	18	24	37
W-50068	238	271	942368	964935	8.0	40	37	25	10	22
W-50069	249	233	904261	954521	18.4	42	38	22	20	20
W-50070	217	236	907002	986074	15.3	48	14	36	12	28
W-50071	206	207	877792	997055	22.7	30	32	23	15	20
W-50072	207	170	840570	996779	25.6	40	35	25	15	30
W-50073	192	170	840529	1011167	27.1	55	20	16	25	19
W-50075	160	154	824758	1043614	28.0	44	18	43	10	12
W-50076	221	181	851555	982583	27.2	48	30	32	12	23
W-50077	231	165	835864	972514	24.3	45	30	32	19	54
W-50078	159	201	872209	1044082	17.5	42	20	38	22	29
W-50079	159	183	853957	1044345	25.9	39	25	26	40	27
W-50080	189	141	811648	1014017	30.5	62	25	17	35	12
W-50081	187	104	775317	1016722	27.5	50	15	20	10	43

APPENDIX B:
HYDROGEOLOGIC CROSS SECTIONS

Hydrogeologic Cross-Section A-A'

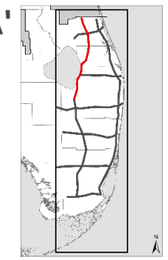

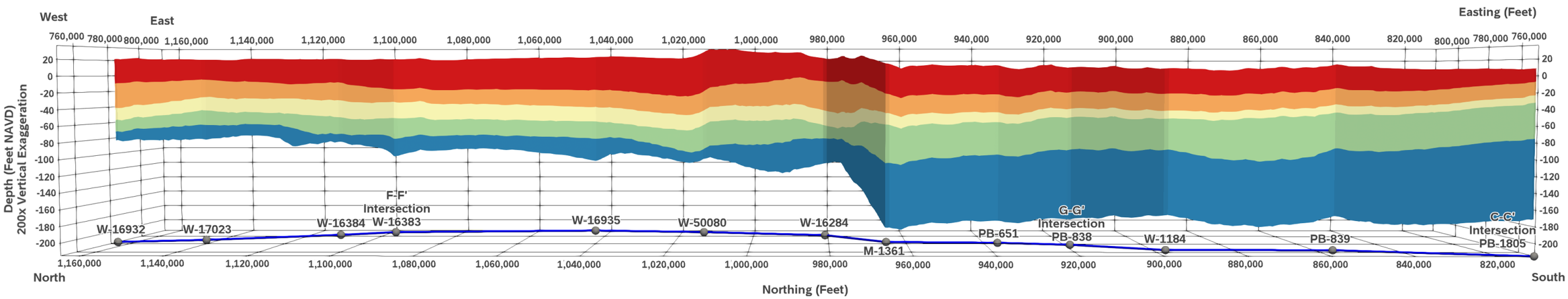

Hydrogeologic Cross-Section B-B'

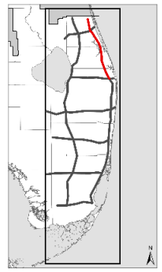

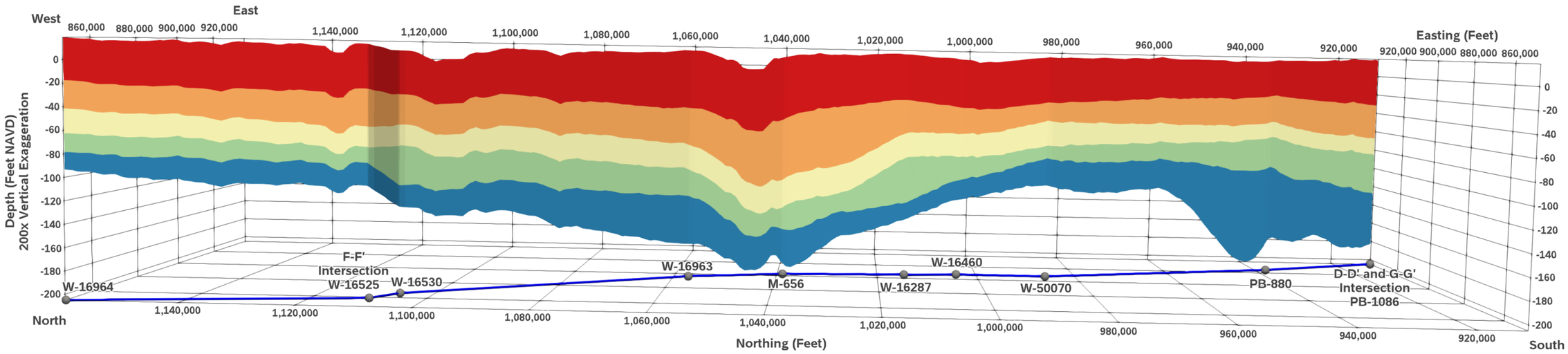

Hydrogeologic Cross-Section C-C'

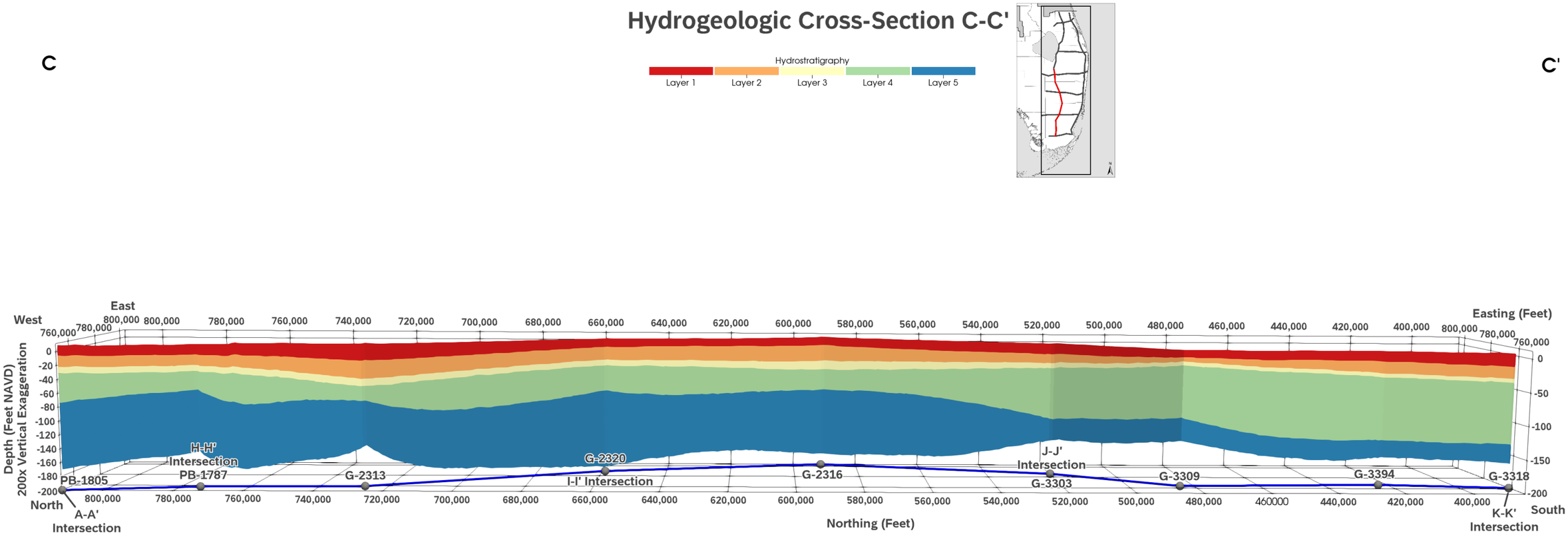

Hydrogeologic Cross-Section D-D'

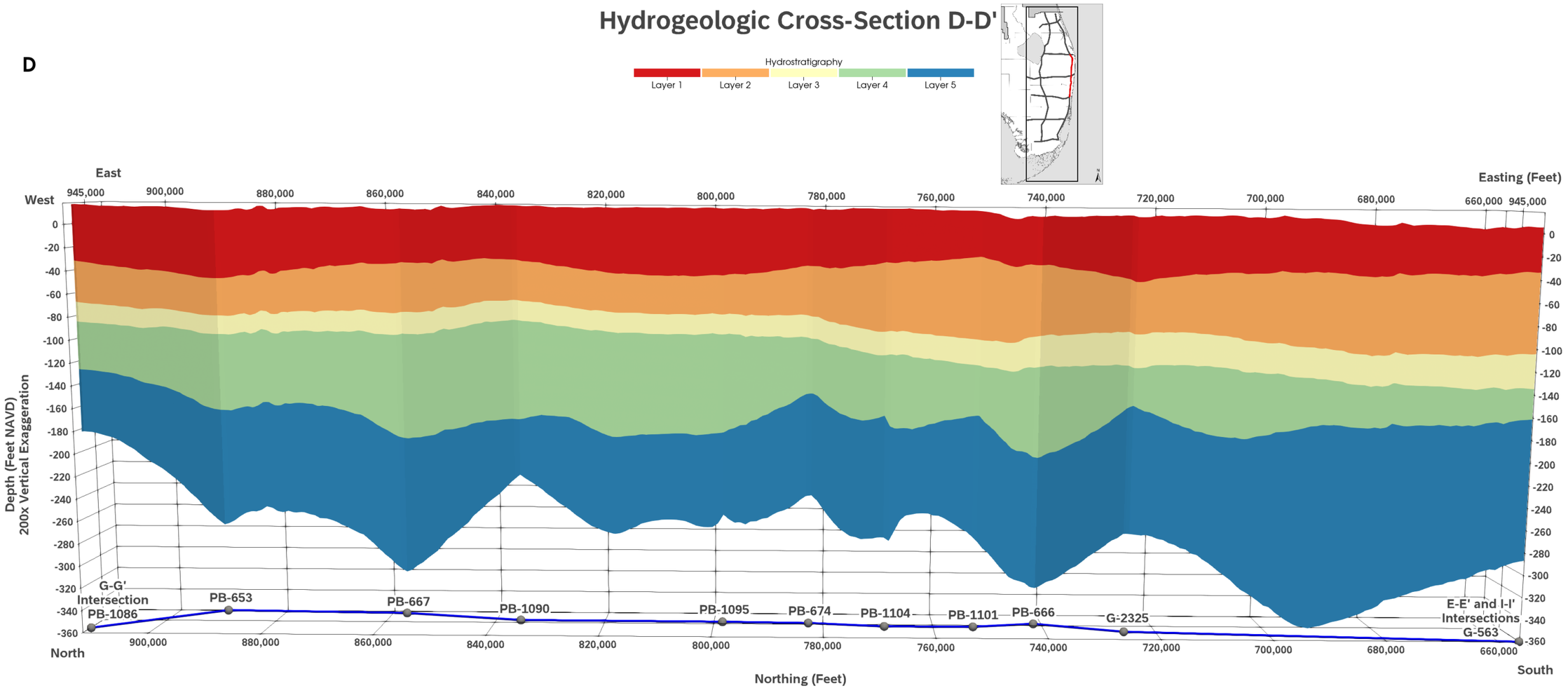

Hydrogeologic Cross-Section E-E'

E

E'

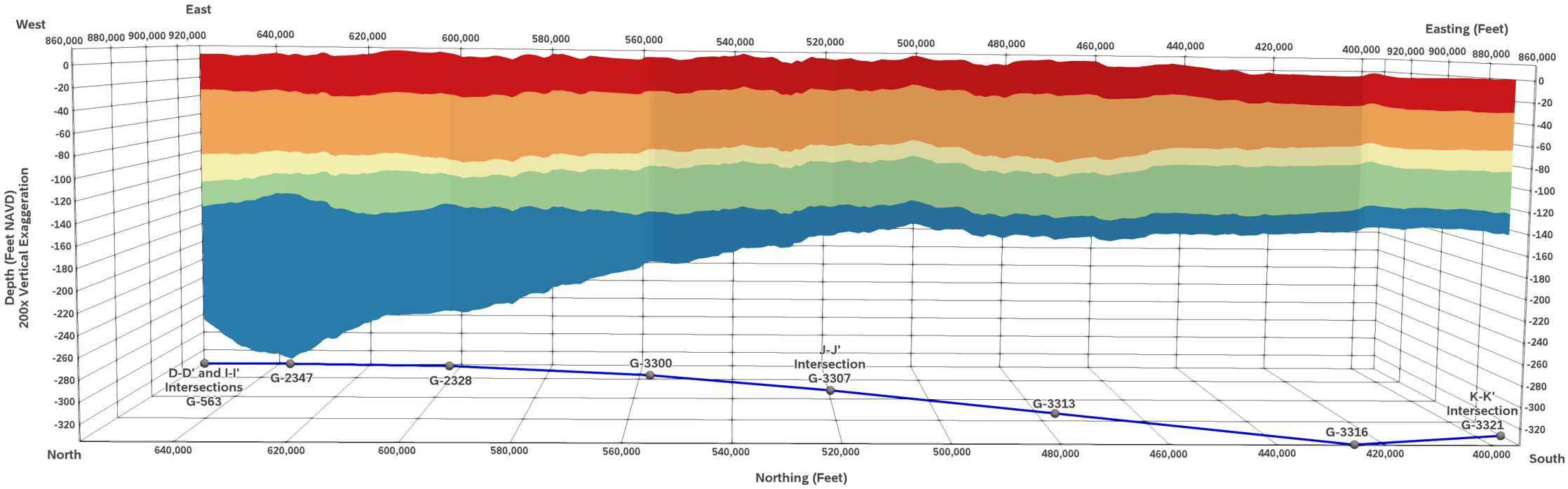

Hydrogeologic Cross-Section F-F'

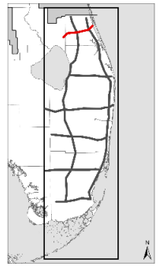

F

F'

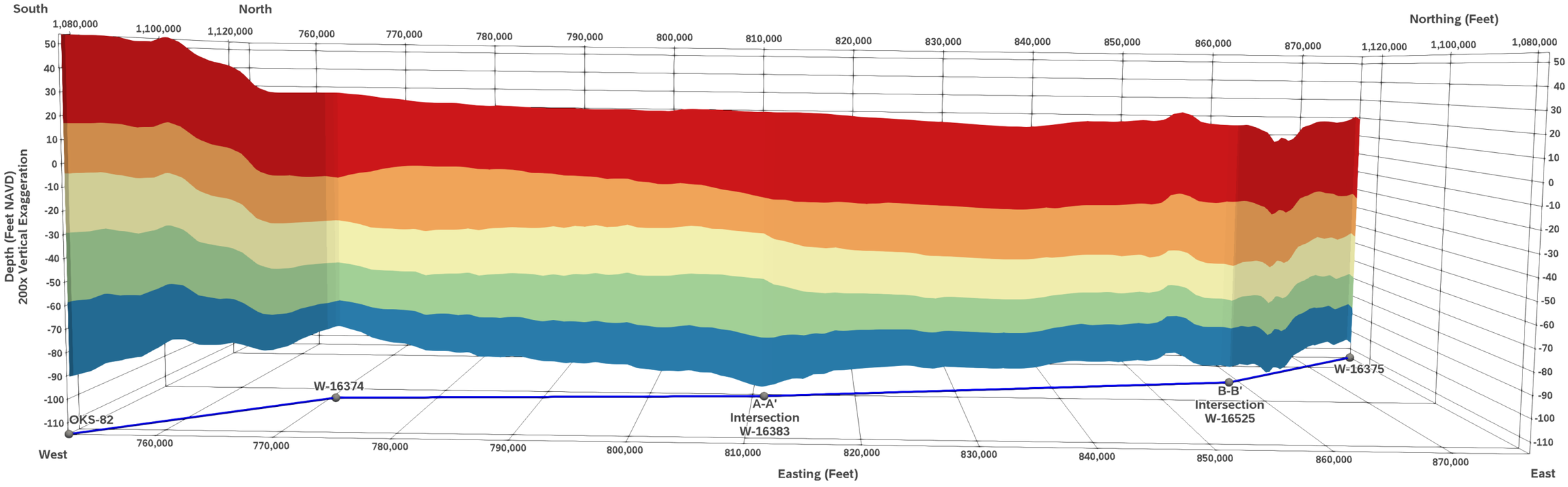

Hydrogeologic Cross-Section G-G'

G

G'

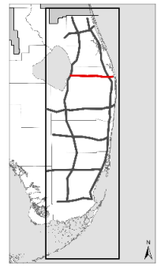

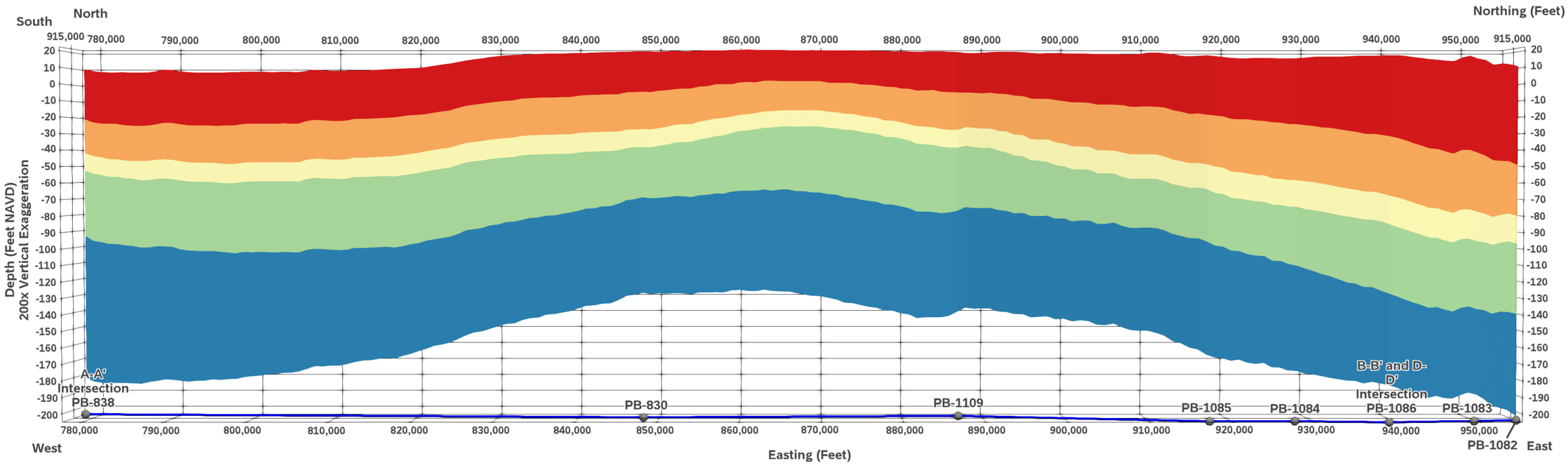

Hydrogeologic Cross-Section H-H'

H

H'

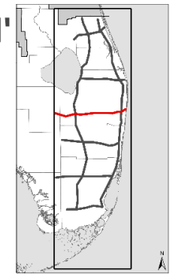

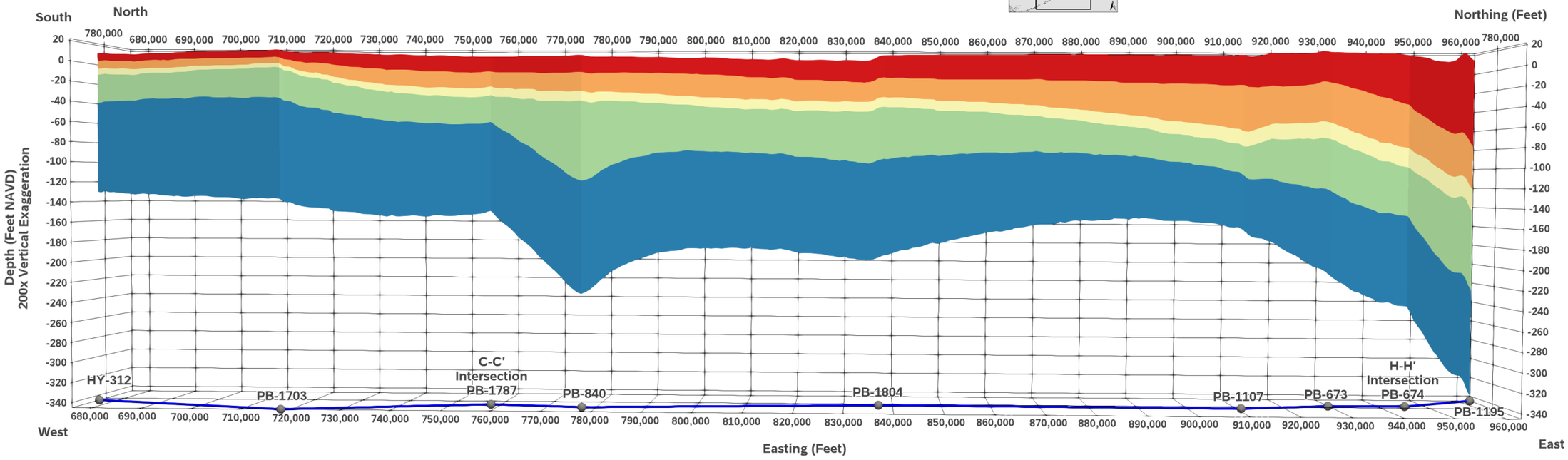

Hydrogeologic Cross-Section I-I'

I

I'

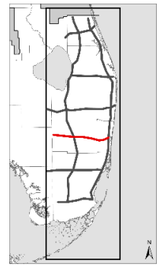

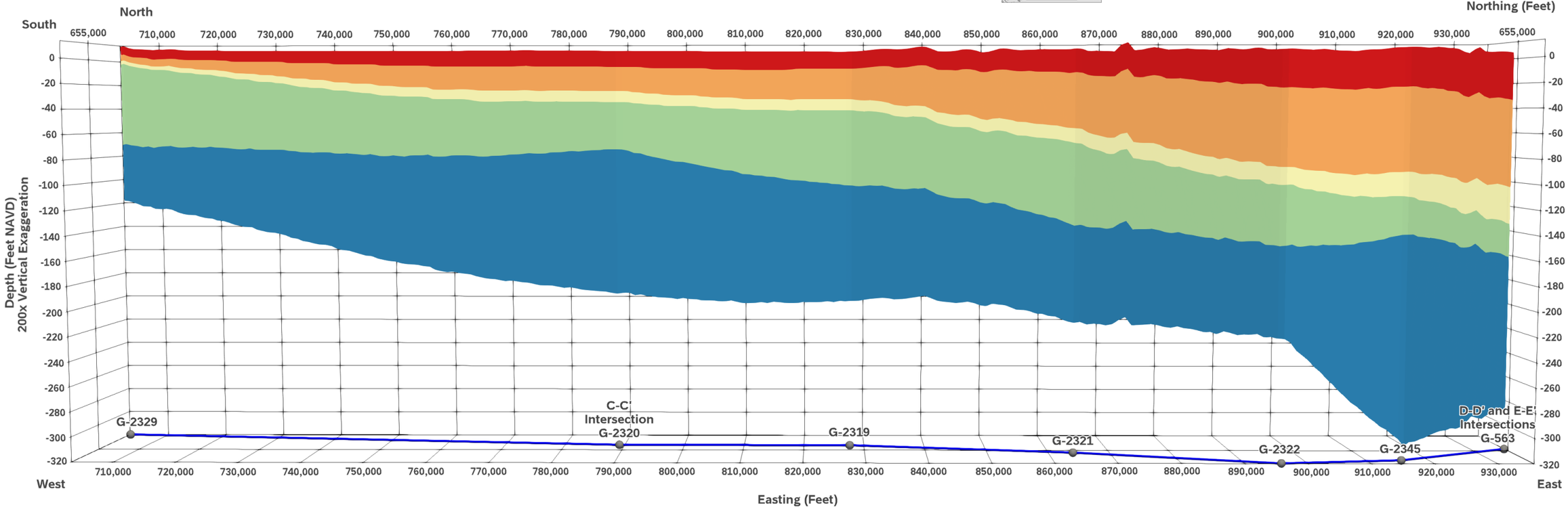

Hydrogeologic Cross-Section J-J'

J

J'

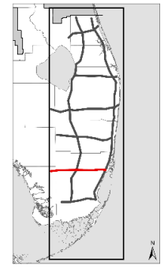

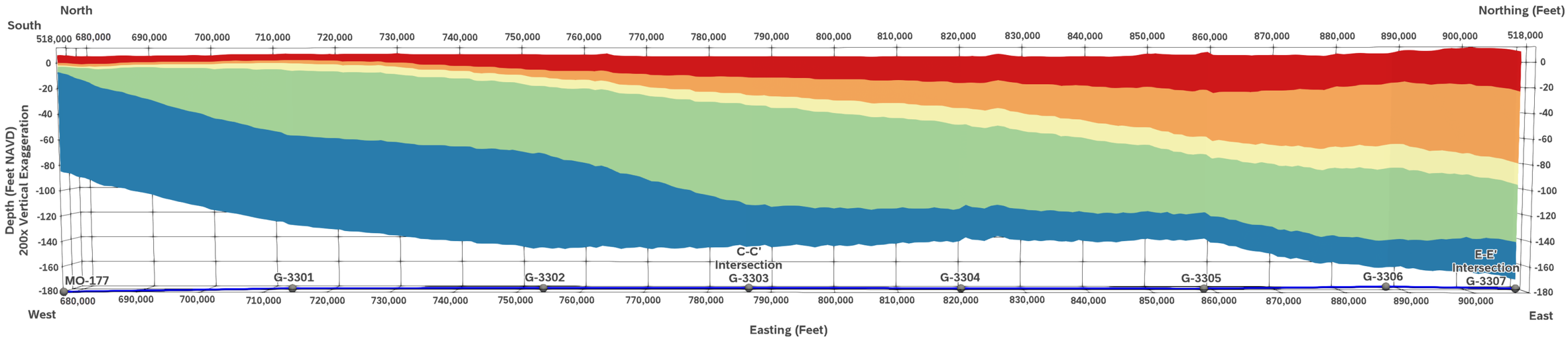

Hydrogeologic Cross-Section K-K'